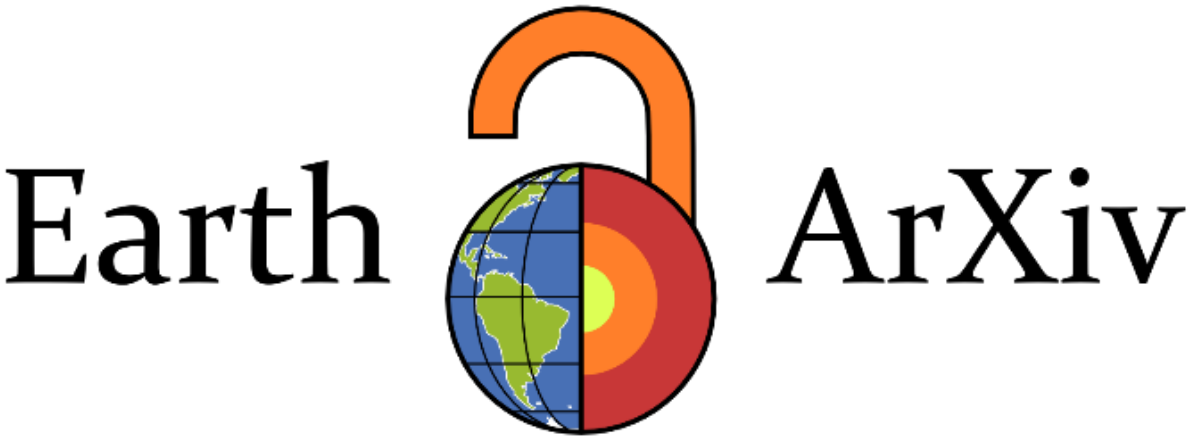

Mineral stabilization of soil organic sulfur at the continental scale

Zhuojun Zhang[1,2], M. Francesca Cotrufo[3], Benjamin L. Turner[4], Hai-Ruo Mao[1], Chao Liang[5], Mohsen Shakouri[6], and Mengqiang Zhu[1,7]*

[1] Department of Ecosystem Science and Management, University of Wyoming, Laramie, Wyoming 82071, United States

[2] State Key Laboratory of Lake and Watershed Science for Water Security, Nanjing Institute of Geography and Limnology, Chinese Academy of Sciences, Nanjing, Jiangsu 211135, China

[3] Department of Soil and Crop Science and Natural Resource Ecology Laboratory, Colorado State University, Fort Collins, Colorado 80523, United States

[4] Institute of Agriculture and Life Sciences, Gyeongsang National University, 501 Jinju-Daero, Jinju 52828, South Korea

[5] Institute of Applied Ecology, Chinese Academy of Sciences, Shenyang, Liaoning 110016, China

[6] Canadian Light Source Inc., University of Saskatchewan, Saskatoon, Saskatchewan S7N 2V3, Canada

[7] Department of geological, Environmental, and Planetary Sciences, University of Maryland, College Park, Maryland 20740, United States

* Corresponding author: Mengqiang Zhu

Email: mqzhu@umd.edu

Running Title: Mineral stabilization of soil organic sulfur

Abstract

Declining atmospheric sulfur (S) deposition makes S an emerging limiting macronutrient to plants, yet the stability and dynamics of soil organic S - the largest terrestrial S pool supplying plant-available sulfate via mineralization - remain unclear. Across North American soils, mineral-associated organic S (MAOS), a stabilized pool by mineral protection, dominates (61 ± 26% of the total soil S) but saturates at ~ 600 μg S g^{-1} soil. Compared with labile particulate organic S (POS) that does not saturate, MAOS is more decomposed, chemically diverse, and climate-sensitive. Projected global warming accelerates S mineralization in both pools, but shifting moisture regimes drive their divergence in supplying available S, with MAOS stabilizing in wetter soils while POS remains labile. This comprehensive reassessment of soil S cycle at the continental scale reveals a mineral "gatekeeper" that both shields organic S and retains sulfate, providing a mechanistic basis for nutrient management and carbon sequestration in response to climate change in a S-scarce future.

Keywords: organic S mineralization, mineral stabilization, S availability, soil S cycle, climate change, organic matter fractions

1 Introduction

Sulfur (S) is a vital macronutrient essential for all life, yet global soils are becoming increasingly deficient in S due to a worldwide decline in atmospheric S deposition (Silvia Haneklaus, Bloem, & Schnug, 2008; Hinckley, Crawford, Fakhraei, & Driscoll, 2020). Soil parent materials are typically low in S, so anthropogenic SO_2 and SO_4^{2-} deposition has served as a major external source since the industrial revolution (S. Haneklaus, Bloem, & Schnug, 2003). However, global S emissions have declined by ~ 40% since 1990, driven by air quality improvements, with reductions approaching 90% in North America and Europe (Feinberg et al., 2021; Ritchie & Roser, 2021). This decline has led to widespread S limitation across natural and agricultural ecosystems,

particularly in arable soils (Hinckley et al., 2020; Messick, Fan, & De Brey, 2005), prompting growing reliance on supplemental S fertilizers to sustain food production (Gerson & Hinckley, 2023; Hinckley et al., 2020). As atmospheric contributions diminish, microbial mineralization of soil organic S – the largest terrestrial S pool and accounting for over 95% of the total soil S (Jørgen Eriksen, 2009; Kovar & Grant, 2011; Niknahad-Gharmakher, Piutti, Machet, Benizri, & Recous, 2012) – has become increasingly important for sustaining plant-available sulfate (Barnard et al., 2025; Churka Blum, Lehmann, Solomon, Caires, & Alleoni, 2013; Fakhraee, Li, & Katsev, 2017; Kovar & Grant, 2011; Tolu et al., 2022). Yet, organic S compounds are not uniformly accessible: associations with soil minerals can stabilize organic S, limiting microbial access and constraining mineralization (J. Eriksen, Murphy, & Schnug, 1998; Solomon, Lehmann, & Martínez, 2003; Tanikawa, Hashimoto, et al., 2014; Tanikawa et al., 2022). The balance between microbial mineralization and mineral stabilization has thus emerged as a central, yet poorly understood, control on terrestrial S cycling.

Traditionally, soil organic S has been categorized by biochemical reactivity into labile ester sulfates (C–OSO_3) and more recalcitrant carbon-bonded S (C–S), with the former presumed more readily mineralized to meet microbial demand (Churka Blum et al., 2013; Edwards, 1998; J. Eriksen et al., 1998; Singh, Rengel, & Bowden, 2006) (Fig. 1). However, mineral associations can strongly modulate these dynamics by physically protecting both compound types from microbial and enzymatic attack (J. Eriksen et al., 1998; Solomon et al., 2003; Tanikawa, Hashimoto, et al., 2014; Tanikawa et al., 2022). Recent developments in soil carbon research offer a mechanistic framework: dividing SOM into particulate organic matter (POM) and mineral-associated organic matter (MAOM) better predicts organic carbon turnover and stability, nitrogen cycling and their responses to climate change (Averill & Waring, 2018; Cotrufo, Ranalli, Haddix, Six, & Lugato, 2019; Lavallee, Soong, & Cotrufo, 2020; Lugato, Lavallee, Haddix, Panagos, & Cotrufo, 2021). Particulate organic matter consists mainly of plant structural residues that decompose on average

on decadal timescales and are stabilized by biochemical and microbial constraints, while MAOM comprises largely of mineral-bound soluble or insoluble compounds of either plant or microbial origin with C turnover times ranging on average from centuries to millennia (Heckman et al.; Lavallee et al., 2020). This conceptual framework has enhanced our understanding of soil carbon persistence and nitrogen availability (Averill & Waring, 2018; Jilling et al., 2018), yet its relevance to soil organic S remains largely unexplored. Although some studies have demonstrated mineral controls on S dynamics in specific soil types (J. Eriksen et al., 1998; Solomon et al., 2003; Tanikawa, Hashimoto, et al., 2014; Tanikawa et al., 2022), the quantities, chemical forms, and environmental sensitivities of mineral-associated organic S (MAOS) versus particulate organic S (POS) remain uncharacterized across disparate ecosystems at broad spatial scales.

Here we present the first continental-scale assessment of physical and chemical nature of soil organic S, extending the MAOM–POM framework to S using samples from 40 sites across 20 U.S. ecoclimatic domains in the National Ecological Observatory Network (NEON). Consistent with the most recent understanding of SOM physical fractions (Leuthold, Lavallee, Haddix, & Cotrufo, 2024), we fractionated SOM by density and size and considered POM as the light (LPOM, < 1.85 g cm^{-3}) and heavy fraction (HPOM, > 1.85 g cm^{-3} & > 53mm), and MAOM as the fine heavy fraction (> 1.85 g cm^{-3} & < 53mm). LPOM and MAOM were directly characterized but HPOM was not due to its low concentration of S. We measured organic S concentrations in the LPOM (LPOS) and MAOM fractions (MAOS) and the bulk soil (TOS). Hereafter, the total particulate organic matter, defined as HPOM + LPOM, is termed POM. Similarly, total particulate organic S contained in combined HPOM and LPOM is denoted as POS, which was estimated as the difference between MAOS and TOS. Further, we characterized S speciation in the MAOM (i.e., MAOS) and LPOM (i.e., LPOS) fractions and the bulk soil using S K-edge X-ray absorption near-edge structure (XANES) spectroscopy. We used average S oxidation state as a proxy for the extent of OS decomposition and applied path analyses to identify climatic, mineralogical, and other edaphic

drivers of S stabilization and decomposition (see Methods for details). Our findings provide new insights into the geochemical architecture of soil organic S and its sensitivity to environmental factors, advancing our ability to manage S fertility and availability in a changing climate.

2 Materials and Methods

2.1 Soil samples and analysis

We used the subsamples of A and B horizons from 40 sites in the NEON Megapit archive. Detailed soil profile descriptions for the NEON sites we studied are provided in Supplementary Table S1. To obtain different fractions of OM, we utilized a physical soil organic matter fractionation scheme as described by Soong and Cotrufo (Soong & Cotrufo, 2015). Briefly, a 5 g subsample of oven-dried bulk soil was dispersed with glass beads in 25 mL of 1.85 g cm^{-3} sodium polytungstate solution (SPT) to disperse all aggregates. Then, the samples were centrifuged, and the light particulate OM (LPOM < 1.85 g cm^{-3}) was aspirated from the sample and rinsed to remove SPT. The remaining heavy fraction was rinsed thoroughly to remove SPT and then sieved through a 53-μm screen to separate the heavy sand-sized OM (HPOM > 1.85 g cm^{-3} and > 53 μm) and mineral associated organic matter (MAOM > 1.85 g cm^{-3} and < 53 μm). All fractions were oven-dried at 60 °C prior to the analysis. The total mass recovery from the fractions was within ±5% of the initial mass.

We directly characterized the LPOM and MAOM fractions, but the HPOM fraction was not directly characterized due to its low S concentration. Organic S concentrations in the LPOM and MAOM fractions and the bulk soil (TOS) were measured using a Thermo Flash Elemental Analyzer. The MAOS concentration in bulk soil was calculated by multiplying the S concentration in MAOM by the mass percentage of MAOM material over total bulk soil. The total particulate organic matter, defined as HPOM + LPOM, is termed POM. Similarly, total particulate organic S contained in combined HPOM and LPOM is denoted as POS, which was estimated as the difference between

MAOS and TOS. The close correlation between LPOS and POS in the topsoil, as indicated by the regression line (Fig. S1), suggests that POS is predominantly derived from LPOS.

Exchangeable S in soils, considered as available S here, was extracted using a 0.016 M KH_2PO_4 solution at a 1:20 ratio. After agitation on a reciprocal shaker for 2 hours, the samples were centrifuged and then filtered through 0.45 μm syringe filters. The filtrates were then analyzed for the SO_4^{2-} concentration by ion chromatography (Dionex ICS-90, Thermo Scientific, Massachusetts, USA).

2.2 Sulfur K-edge XANES spectroscopy

Sulfur K-edge XANES spectra were collected from bulk soil, LPOM and MAOM in the top A and B horizons at the Soft X-ray Micro-Characterization Beamline (SXRMB) at the Canadian Light Source, Saskatoon, Canada. XANES spectra for all samples were recorded in fluorescence yield using a 7-element SDD detector (RaySpec Inc.) over the energy range of 2442–2542 eV. Measurements were conducted in three segments: 2442–2466 eV with 2 eV steps, 2466–2497 eV with 0.15 eV steps, and 2497–2542 eV with 0.75 eV steps. The X-ray energy was calibrated to the K-edge of elemental S at 2472.7 eV. The XANES spectra data were merged and normalized using the software ATHENA. The spectra were further fitted using a series of Gaussian functions (G1, G2, G3, G4, and G5) and two arctangent functions (step height) following the approach by Wojdyr (2010) using Fityk. The five Gaussian curves correspond to different S species: exocyclic S (G1), heterocyclic S (G2), sulfoxide (G3), sulfonate (G4), and inorganic and ester SO_4^{2-} (G5) (Prietzel et al., 2011). The relative abundance of each S functional group was calculated from the area under the respective Gaussian peak relative to the total area under all the Gaussian peaks. The areas were corrected for energy-dependent absorption cross section using the generic calibration curve (Manceau & Nagy, 2012):

$$y = 0.36841x - 909.97$$

where x is the white-line peak energy and y is the scaling factor normalized to y = 1 at the energy of elemental S (E 2472.70 eV). It has been reported that the error for the OS fraction with the Gaussian curve fit is 4-8% for reduced and < 5% for oxidized S species (Huffman et al., 1991; Manceau & Nagy, 2012).

The electronic oxidation state (EOS) of each S species was calculated using the equation (Zeng, Arnold, & Toner, 2013):

$$EOS = 0.6179x - 1529$$

where x is the white-line peak energy. In this study, EOS values were reported as calculated for the low-valent S species (EOS ≤+4) and EOS values were rounded to integer values for the high-valent S species (EOS >+4). The average electronic oxidation state (ASOX) of S was calculated using the following equation:

$$ASOX=EOS_{G1} \times F_{G1}+ EOS_{G2} \times F_{G2}+ EOS_{G3} \times F_{G3}+ EOS_{G4} \times F_{G4}+ EOS_{G5} \times F_{G5}$$

where F represents the proportion of each fraction.

2.3 Statistical analyses

Structural equation modeling (SEM) was used to explore the direct and indirect effects of climatic and edaphic variables on the concentrations of MAOS and POS, exchangeable S concentration and percentage, as well as average S oxidation states (ASOX) in bulk soil, LPOM and MAOM. Multiple goodness-of-fit tests were applied, including the Chi-square/degree of freedom (c^2/df) test ($p > 0.05$), the comparative fit index (CFI > 0.9), and the root mean square error of approximation (RMSEA < 0.08). The path coefficient (l) for each environmental factor indicated its effects on the target variable. The R^2 values represented the proportion of the variance explained by the variables. The total effects were obtained by multiplying the l values along the related effect paths and summing them. The SEM analyses were conducted using AMOS 22.0 (Amos Development Co.).

All the correlation analyses in this study were conducted using Origin 2018. To evaluate the significance of these relationships, a one-way analysis of variance (ANOVA) method was applied. The relationships between TOS and concentrations of MAOS and POS were fitted using asymptotic and ExpDec models, respectively. All other correlations were fitted using ordinary least squares linear regression.

3 Results and Discussion

3.1 Distributions of MAOS and POS

We find that MAOS constitutes a substantial fraction of total organic S across North American soils, though its contribution varied considerably across sites (Figs. 2a–b). In the surface (A) horizon, mean (± SD) concentrations of TOS, MAOS, and POS were 312 ± 294, 155 ± 124, and 157 ± 259 μg/g soil, respectively, declining to 187 ± 231, 88 ± 84, and 99 ± 199 μg/g soil in the B horizon (Fig. 2a). The fraction of MAOS relative to TOS (f_{MAOS}) averaged 57 ± 21% in the A horizon soil and 64 ± 28% in the B horizon (subsurface), without significant difference between the two horizons (Fig. 2b). On average, mineral-associated S accounted for 61 ± 26% of total organic S across all samples, underscoring the widespread role of mineral stabilization in shaping soil organic S pools and MAOM as a major S reservoir larger than POM on average. Notably, the concentrations of TOS, MAOS, and POS as well as f_{MAOS} did not differ significantly among ecosystem types (Figs. S2a–d), suggesting common underlying mechanisms governing S partitioning across ecosystems although the different numbers of data points for each ecosystem type may obscure the finding.

Despite this broad prevalence, the capacity of soils to stabilize organic S through mineral associations appears finite. MAOS concentrations exhibit a saturation response with increasing TOS: at low TOS levels, sulfur was primarily stored as MAOS (Fig. 2c), but beyond ~600 μg/g soil, MAOS reached an apparent upper limit, and further increases in TOS occurred exclusively via

POS accumulation (Fig.2d). This saturation pattern closely parallels that of mineral-associated organic carbon (MAOC; Fig. S3) (Cotrufo & Lavallee, 2022; Cotrufo et al., 2019), as expected given the consistently narrow carbon-to-sulfur (C/S) ratios in MAOM (Fig. 2h). However, confirming the saturation threshold requires future empirical work, such as isotopic tracing and controlled S enrichment studies, to assess incorporation rates and stabilization capacity.

Our findings reveal that S availability and mineral interactions may jointly stabilize organic C in soils, underscoring the potential biogeochemical coupling of OS to OC. A comparison of C/S ratios between MAOM and POM suggests that S availability might constrain the formation of MAOC. Similar to C/N, MAOM consistently exhibited lower and less variable C/S ratios than POM (Figs. 2h–i), reflecting more advanced microbial processing, a higher S demand for MAOM formation (Kirkby et al., 2013), and a stronger affinity for S-rich organic molecules for soil mineral surfaces (Spohn, 2024). Soils with higher f_{MAOC} tended to show higher C/S ratios in MAOM (Fig. S8), suggesting more efficient S use in carbon stabilization under S-limited conditions. These patterns imply that, like nitrogen and phosphorus (Favaro, Carrillo, Singh, Warren, & Dijkstra, 2025; Lieberman, von Sperber, & Kallenbach, 2025; Spohn, 2020), sulfur can act as a limiting factor in long-term SOC stabilization — an effect likely to intensify as atmospheric S inputs continues to decline. The close relationship between organic C and S is further supported by strong correlations between MAOC and MAOS, and between POC and POS (Figs. 2e–f, 3a–b). MAOS and POS concentrations were elevated in soils with higher C/N ratios of MAOM and POM and in cooler climates (Figs. 3a–b), suggesting potential S enrichment in less decomposed organic matter. This likely reflects the relative stability of C-bonded S in fresher material compared to ester-bound S in more processed compounds. Mineralogical controls were especially important for MAOS: both silt/clay content and oxalate-extractable Fe and Al were positively associated with MAOS concentrations (Fig. 3a), highlighting the role of secondary minerals in organic S accumulation and stabilization. Higher effective soil moisture may further enhance MAOS accrual, likely by

196 stimulating mineral weathering and plant productivity, while lower pH may suppress microbial
197 processing and necromass stabilization. Among all variables, the fraction of MAOC (f_{MAOC})
198 emerged as the strongest predictor of the proportion of MAOS in total organic S (f_{MAOS}; Fig. 3c),
199 reinforcing the conclusion that C and S are potentially co-stabilized through mineral associations
200 under warm, moist, and mineral-rich conditions. Future studies are warranted to determine the
201 specific mechanisms by which S availability and mineral interactions drive organic C stabilization.

202 **3.2 Oxidation states and decomposition of MAOS and POS**

203 The chemical composition of organic S varied widely across the continent and differed
204 significantly between MAOS and LPOS, though not among ecosystems (Figs. 4A; Figs. S2j–r).
205 Light POS in the A horizon was dominated by C-bonded S (89% ± 4%) with little ester sulfate (11%
206 ± 4%), whereas MAOS exhibited lower C-bonded S (73% ± 13%) and higher ester sulfate (27% ±
207 13%) with greater variability (as shown by higher standard deviations) than POS, reflecting a more
208 oxidized and decomposed state of MAOS. This greater variability suggests that MAOS is more
209 chemically sensitive than LPOS to environmental conditions. Our finding is consistent with that
210 organic S is more oxidized in clay fractions than in bulk soils (Prietzel, Thieme, Salomé, & Knicker,
211 2007). Despite being closer to complete mineralization on average, MAOS is expected to be more
212 stable due to mineral protection, particularly for ester sulfate through strong adsorption of its SO_4^{2-}
213 group onto mineral surfaces, slowing further mineralization (Prietzel et al., 2007; Tanikawa,
214 Noguchi, et al., 2014; Yang et al., 2016).

215 The contrasting compositions of MAOS and LPOS reflect differences in the origin and
216 transformation of MAOM and LPOM. The high C-bonded S content in LPOM aligns with its
217 predominantly plant-derived origins, as plants primarily contribute C-bonded S. Oxidation of this
218 C-bonded S produces ester sulfate, which can then hydrolyze rapidly to release inorganic sulfate
219 without subsequent mineral protection, which further enriches C-bonded S in LPOM relative to

ester sulfate. Microbial residues, especially those from fungi that are rich in ester sulfate (Heinze et al., 2021), may also contribute to the ester sulfate content of LPOM. In contrast, MAOM accrues more ester sulfate, likely due to multiple mechanisms such as preferential adsorption of ester sulfate to mineral surfaces via its SO_4^{2-} group, greater microbial decomposition, and higher microbial (fungal) residue inputs. The higher ester sulfate proportion in B horizon soils (Fig. 4Ab) further supports the role of mineral surfaces, particularly secondary minerals abundant in deeper layers, in concentrating and stabilizing ester sulfate.

Environmental conditions, especially temperature and effective soil moisture, appear to further shape the chemical state and stability of organic S pools. Path analyses identified MAT, MAP – PET, and soil pH (itself influenced by MAP – PET; Fig. S7b) as potential key drivers. MAT positively correlated with the oxidation states of both MAOS and LPOS, with stronger effects in the B horizon than the A horizon (Figs. 4Ba–e, Figs. 3d–h), consistent with evidence that warming accelerates organic matter decomposition more in subsoils (Jia et al., 2019; Ofiti et al., 2021). In contrast, MAP – PET had divergent effects on the two S pools (Figs. 4Bf–j, Figs. 3d–h). LPOS oxidation increased slightly with MAP – PET, likely due to enhanced decomposition in wetter but oxygen-rich macropores hosting LPOM, though this effect might be tempered by lower pH at high moisture. MAOS oxidation, however, declined markedly with increasing MAP – PET, especially in the A horizon. This trend reflects enhanced anoxia and acidification in micropores hosting MAOM, which limit microbial oxidation and preserve reduced S forms (Keiluweit, Wanzek, Kleber, Nico, & Fendorf, 2017; Zhu et al., 2026). Increased leaching under wetter conditions also transports less-decomposed, plant-derived compounds into mineral soils, further enriching MAOM in reduced organic S (Chakrawal, Lindahl, Qafoku, & Manzoni, 2024; Christ & David, 1996). Compared to the A horizon, the B horizon showed weaker correlations with MAP – PET, likely due to lower SOC and water concentration that disfavor development of reducing soil conditions. Overall, these results demonstrate how climate-driven variations in temperature and moisture

modulate organic S oxidation and stabilization, with implications for the persistence of organic S and release of plant-available sulfate in soils.

3.3 Sulfate availability in soils

Sulfur availability in soils, typically measured as exchangeable S, averaged 12 ± 13 μg/g soil in the A horizon and 41 ± 80 μg/g soil in the B horizon (Fig. 5a). The proportion of exchangeable S relative to total S ($f_{exc\ S}$) was also higher in the B horizon (20 ± 21%) than in the A horizon (5 ± 6%) (Fig. 5b). Both the concentration and proportion of exchangeable S were consistently greater in forest ecosystems compared to grasslands (Figs. S2e, f), suggesting enhanced S availability under forest cover.

Exchangeable S in soils is influenced by climatic conditions and soil mineralogy, with positive correlations with MAP – PET and oxalate-extracted Fe and Al (Fig. 5c). The strong association with Fe and Al underscores the role of sulfate adsorption to metal oxides, which explains the higher exchangeable S levels in the B horizon and in forest soils, where these oxides are more abundant (Figs. 5a; S2e). MAP – PET likely enhances exchangeable S by promoting Fe/Al oxide formation and increasing wet atmospheric sulfate deposition, though dry deposition, which may also contribute (Luo et al., 2016), was not considered in this study.

Beyond environmental drivers, the size and oxidation state of organic S pools may play key roles in S availability. Exchangeable S was positively correlated with LPOS concentration and the oxidation state of MAOS, but negatively with the oxidation state of LPOS (Fig. 5c). The link to LPOS may reflect its high lability and rapid turnover, which readily releases sulfate into the exchangeable pool. The negative correlation with the oxidation state of LPOS likely reflects loss of ester sulfate through hydrolysis, which both lowers its oxidation state and contributes sulfate to the exchangeable pool. That is, oxidative decomposition of LPOS is an important source of exchangeable sulfate. In contrast, the positive correlation with the oxidation state of MAOS

suggests that ester sulfate-rich MAOS, although stabilized by mineral associations, can gradually release sulfate over time through enzymatic mineralization following MAOM destabilization. The same factors and mechanisms influencing exchangeable S concentrations also apply to its proportion relative to total S, except that POS concentration and Fe/Al oxides showed much weaker effects (Fig. 5d). Overall, oxidation states of organic S seem to exert a stronger influence than pool sizes on exchangeable sulfate. This finding suggests that the degree of organic matter decomposition is a more critical regulator of S availability than the absolute amount of organic S although atmospheric deposition of sulfate may obscure the conclusion.

3.4 Role of minerals in sustaining sulfur fertility in soils

Our findings indicate that minerals in the silt and clay fractions exert dual control on soil S availability. On one hand, mineral associations concentrate organic S in MAOM and protect it from microbial decomposition, particularly organic sulfate, presumably slowing down the release of inorganic sulfate for biological uptake. On the other hand, the same minerals adsorb sulfate with moderate binding strength, reducing leaching while maintaining its plant availability (J. Eriksen & Askegaard, 2000). Elevated exchangeable sulfate in clay-rich soils therefore indicates that, despite protection, MAOS continues to mineralize slowly because of MAOM destabilization and subsequent mineralization (Bölscher et al., 2025; Jilling et al., 2025); the released sulfate is efficiently retained on mineral surfaces and accumulates over time. Inorganic sulfate from mineralization of POS and atmospheric deposition also enhances the adsorbed sulfate pool in soils. Consequently, sulfate deficiency is common in sandy soils where low adsorption capacity facilitates organic S mineralization and subsequent sulfate leaching, but rare in fine-textured soils (Edwards, 1998). Thus, minerals function as sustained slow-release agents of plant-available sulfate in soils.

3.5 Implications for sulfur nutrient management

Our results predict that projected warming accelerates S mineralization in both organic S pools but shifting moisture regimes drive their divergence in supplying available S. Ignoring these differences of the two pools in responses to climate change would lead to inaccurate predictions and poor management strategies. Our findings suggest that in those warmer, drier regions (Dai, 2013), sulfate release from MAOS increases, heightening the risk of S leaching into aquatic ecosystems, which can trigger severe environmental cascades such as mercury methylation, eutrophication, and sulfide toxicity to native flora and fauna (Lamers et al., 2002; Regnell & Watras, 2019; Smolders & Roelofs, 1993; Wang & Chapman, 1999). In contrast, wetter terrestrial ecosystems (O'Gorman, 2015) sequester more S in MAOS. In these areas, native plant communities may face limited S availability, relying heavily on seasonal wet–dry cycles or climate-driven hydrological shifts to sustain sulfate availability (Liu et al., 2021).

While derived from natural ecosystems, our findings offer a framework for targeted fertility management in agricultural systems that leverages both POS and MAOS pools through practices tailored to soil texture. In coarse, sandy soils, organic inputs (e.g., crop residues, cover crops, and compost) build a labile POS pool for timely sulfate release (Barnard et al., 2025; Cardelli, Saviozzi, Cipolli, & Riffaldi, 2008; Hansen, Eriksen, Jensen, Thorup-Kristensen, & Magid, 2021; Piutti et al., 2015), while Fe- and Al-rich amendments or biochar expand MAOS, and retain sulfate and limit its leaching (Ding et al., 2016; Lei et al., 2024; Penn, Bryant, Callahan, & McGrath, 2011). Conversely, fine-textured (clay-rich) soils require moderate aeration and controlled MAOS turnover (via brief drainage or shallow fertilizer banding) to release sulfate without depleting long-term S reserves (Tariq et al., 2018; Zheng et al., 2024). Notably, any S management strategy must be balanced with carbon sequestration goals. Because the mineral surfaces that stabilize MAOS also protect SOC, aggressively mobilizing sulfate can oxidize stored carbon, whereas maximizing SOC storage (e.g., via clay addition or no-till) can immobilize S and induce deficiencies(Janzen, 2006; Wright & Hons, 2005). Thus, an optimal strategy is to maintain a predominantly MAOC–

MAOS matrix while creating localized, temporal hotspots of S mineralization (through banded fertilizer, rhizosphere redox shifts, or strip tillage) (Battisti, Zavattaro, Capo, & Blandino, 2022; Bölscher et al., 2025; Brainard, Peachey, Haramoto, Luna, & Rangarajan, 2013; Tauchnitz, Bischoff, Schrödter, Ebert, & Meissner, 2018) so that roots capture released sulfate and prevent S deficiencies from undermining carbon sequestration efforts.

Author Contributions

Z.Z. conceptualized the study, performed experiments and data collection and analysis. M.F.C. provided MAOM samples. H.-R.M. conducted structural equation modeling analysis. M.S. collected S XANES data. M.Z. initiated and conceptualized the study, secured funding, and supervised the project. Z.Z. and M.Z. co-wrote the manuscript, and all authors contributed to editing and revision.

Acknowledgments

This work was partially supported by the U.S. National Science Foundation under DEB 2027284 and EAR-1752903. We thank Rebecca Even (Colorado State University) for her assistance in MAOM separation. The National Ecological Observatory Network (NEON) is a program sponsored by the U.S. National Science Foundation and operated under cooperative agreement by Battelle. Sulfur K-edge XANES measurements were performed at the SXRMB beamline at the Canadian Light Source (CLS), a national research facility of the University of Saskatchewan, which is supported by the Canada Foundation for Innovation (CFI), the Natural Sciences and Engineering Research Council (NSERC), the National Research Council (NRC), the Canadian Institutes of Health Research (CIHR), the Government of Saskatchewan, and the University of Saskatchewan.

Competing Interest Statement

The authors declare that they have no conflict of interest.

References

Averill, C., & Waring, B. 2018. "Nitrogen limitation of decomposition and decay: How can it occur?". *Global Change Biology, 24*(4), 1417-1427.

Barnard, M., McKenna, B. A., Dalal, R. C., et al. 2025. "Sulfur's long game: 145 years of soil sulfur speciation in the world's oldest agricultural experiments". *Global Change Biology, 31*(3), e70136.

Battisti, M., Zavattaro, L., Capo, L., et al. 2022. "Maize response to localized mineral or organic NP starter fertilization under different soil tillage methods". *European Journal of Agronomy, 138*, 126534.

Bölscher, T., Cardon, Z. G., Garcia Arredondo, M., et al. 2025. "Vulnerability of mineral-organic associations in the rhizosphere". *Nature Communications, 16*(1), 5527.

Brainard, D. C., Peachey, R. E., Haramoto, E. R., et al. 2013. "Weed ecology and nonchemical management under strip-tillage: implications for northern U.S. vegetable cropping systems". *Weed Technology, 27*(1), 218-230.

Cardelli, R., Saviozzi, A., Cipolli, S., et al. 2008. "Compost and cattle manure as sources of inorganic sulphur to soil". *Archives of Agronomy and Soil Science, 54*(2), 139-147.

Chakrawal, A., Lindahl, B. D., Qafoku, O., et al. 2024. "Comparing plant litter molecular diversity assessed from proximate analysis and 13C NMR spectroscopy". *Soil Biology and Biochemistry, 197*, 109517.

Christ, M. J., & David, M. B. 1996. "Temperature and moisture effects on the production of dissolved organic carbon in a Spodosol". *Soil Biology and Biochemistry, 28*(9), 1191-1199.

Churka Blum, S., Lehmann, J., Solomon, D., et al. 2013. "Sulfur forms in organic substrates affecting S mineralization in soil". *Geoderma, 200-201*, 156-164.

Cotrufo, M. F., & Lavallee, J. M. 2022. Chapter One - Soil organic matter formation, persistence, and functioning: A synthesis of current understanding to inform its conservation and regeneration. In D. L. Sparks (Ed.), *Advances in agronomy* (Vol. 172, pp. 1-66): Academic Press.

Cotrufo, M. F., Ranalli, M. G., Haddix, M. L., et al. 2019. "Soil carbon storage informed by particulate and mineral-associated organic matter". *Nature Geoscience, 12*(12), 989-994.

Dai, A. 2013. "Increasing drought under global warming in observations and models". *Nature Climate Change, 3*(1), 52-58.

Ding, Y., Liu, Y., Liu, S., et al. 2016. "Biochar to improve soil fertility. A review". *Agronomy for Sustainable Development, 36*(2), 36.

Edwards, P. J. 1998. "Sulfur cycling, retention, and mobility in soils: a review".

Eriksen, J. 2009. Chapter 2 Soil sulfur cycling in temperate agricultural systems. In *Advances in agronomy* (Vol. 102, pp. 55-89): Academic Press.

Eriksen, J., & Askegaard, M. 2000. "Sulphate leaching in an organic crop rotation on sandy soil in Denmark". *Agriculture, Ecosystems & Environment, 78*(2), 107-114.

Eriksen, J., Murphy, M. D., & Schnug, E. 1998. The soil sulphur cycle. In E. Schnug (Ed.), *Sulphur in Agroecosystems* (pp. 39-73). Dordrecht: Springer Netherlands.

Fakhraee, M., Li, J., & Katsev, S. 2017. "Significant role of organic sulfur in supporting sedimentary sulfate reduction in low-sulfate environments". *Geochimica et Cosmochimica Acta, 213*, 502-516.

Favaro, A., Carrillo, Y., Singh, B., et al. 2025. "Nutrient-rich mineral-associated organic matter limits carbon storage under elevated carbon dioxide in a low phosphorus Eucalyptus woodland soil". *Global Change Biology, 31*(11), e70585.

Feinberg, A., Stenke, A., Peter, T., et al. 2021. "Reductions in the deposition of sulfur and selenium to agricultural soils pose risk of future nutrient deficiencies". *Communications Earth & Environment, 2*(1), 101.

Gerson, J. R., & Hinckley, E.-L. S. 2023. "It Is time to develop sustainable management of agricultural sulfur". *Earth's Future, 11*(11), e2023EF003723.

Haneklaus, S., Bloem, E., & Schnug, E. 2003. The global sulphur cycle and its links to plant environment. In Y. P. Abrol & A. Ahmad (Eds.), *Sulphur in Plants* (pp. 1-28). Dordrecht: Springer Netherlands.

Haneklaus, S., Bloem, E., & Schnug, E. 2008. History of sulfur deficiency in crops. In *Sulfur: A Missing Link between Soils, Crops, and Nutrition* (pp. 45-58).

Hansen, V., Eriksen, J., Jensen, L. S., et al. 2021. "Towards integrated cover crop management: N, P and S release from aboveground and belowground residues". *Agriculture, Ecosystems & Environment, 313*, 107392.

Heckman, K., Hicks Pries, C. E., Lawrence, C. R., et al. "Beyond bulk: Density fractions explain heterogeneity in global soil carbon abundance and persistence". *Global Change Biology, 28*(3), 1178-1196.

Heinze, S., Hemkemeyer, M., Schwalb, S. A., et al. 2021. "Microbial Biomass Sulphur—An Important Yet Understudied Pool in Soil". *Agronomy, 11*(8), 1606.

Hinckley, E.-L. S., Crawford, J. T., Fakhraei, H., et al. 2020. "A shift in sulfur-cycle manipulation from atmospheric emissions to agricultural additions". *Nature Geoscience, 13*(9), 597-604.

Huffman, G. P., Mitra, S., Huggins, F. E., et al. 1991. "Quantitative analysis of all major forms of sulfur in coal by x-ray absorption fine structure spectroscopy". *Energy & Fuels, 5*(4), 574-581.

Janzen, H. H. 2006. "The soil carbon dilemma: Shall we hoard it or use it?". *Soil Biology and Biochemistry, 38*(3), 419-424.

Jia, J., Cao, Z., Liu, C., et al. 2019. "Climate warming alters subsoil but not topsoil carbon dynamics in alpine grassland". *Global Change Biology, 25*(12), 4383-4393.

Jilling, A., Grandy, A. S., Daly, A. B., et al. 2025. "Evidence for the existence and ecological relevance of fast-cycling mineral-associated organic matter". *Communications Earth & Environment, 6*(1), 690.

Jilling, A., Keiluweit, M., Contosta, A. R., et al. 2018. "Minerals in the rhizosphere: overlooked mediators of soil nitrogen availability to plants and microbes". *Biogeochemistry, 139*(2), 103-122.

Keiluweit, M., Wanzek, T., Kleber, M., et al. 2017. "Anaerobic microsites have an unaccounted role in soil carbon stabilization". *Nature Communications, 8*(1), 1771.

Kirkby, C. A., Richardson, A. E., Wade, L. J., et al. 2013. "Carbon-nutrient stoichiometry to increase soil carbon sequestration". *Soil Biology and Biochemistry, 60*, 77-86.

Kovar, J. L., & Grant, C. A. 2011. Nutrient Cycling in Soils: Sulfur. In *Soil Management: Building a Stable Base for Agriculture* (pp. 103-115).

Lamers, L. P. M., Falla, S.-J., Samborska, E. M., et al. 2002. "Factors controlling the extent of eutrophication and toxicity in sulfate-polluted freshwater wetlands". *Limnology and Oceanography, 47*(2), 585-593.

Lavallee, J. M., Soong, J. L., & Cotrufo, M. F. 2020. "Conceptualizing soil organic matter into particulate and mineral-associated forms to address global change in the 21st century". *Global Change Biology, 26*(1), 261-273.

Lei, K., Dai, W., Wang, J., et al. 2024. "Biochar and straw amendments over a decade divergently alter soil organic carbon accumulation pathways". *Agronomy, 14*(9), 2176.

Leuthold, S., Lavallee, J. M., Haddix, M. L., et al. 2024. "Contrasting properties of soil organic matter fractions isolated by different physical separation methodologies". *Geoderma, 445*, 116870.

Lieberman, H. P., von Sperber, C., & Kallenbach, C. M. 2025. "Soil phosphorus dynamics are an overlooked but dominant control on mineral-associated organic matter". *Global Change Biology, 31*(7), e70307.

Liu, Q., Romani, M., Wang, J., et al. 2021. "Alternating wet–dry cycles rather than sulfate fertilization control pathways of methanogenesis and methane turnover in rice straw-amended paddy soil". *Environmental Science & Technology, 55*(17), 12075-12083.

Lugato, E., Lavallee, J. M., Haddix, M. L., et al. 2021. "Different climate sensitivity of particulate and mineral-associated soil organic matter". *Nature Geoscience*.

Luo, W., Dijkstra, F. A., Bai, E., et al. 2016. "A threshold reveals decoupled relationship of sulfur with carbon and nitrogen in soils across arid and semi-arid grasslands in northern China". *Biogeochemistry, 127*(1), 141-153.

Manceau, A., & Nagy, K. L. 2012. "Quantitative analysis of sulfur functional groups in natural organic matter by XANES spectroscopy". *Geochimica et Cosmochimica Acta, 99*, 206-223.

Messick, D., Fan, M., & De Brey, C. 2005. "Global sulfur requirement and sulfur fertilizers". *FAL—Agric Res, 283*, 97-104.

Niknahad-Gharmakher, H., Piutti, S., Machet, J. M., et al. 2012. "Mineralization-immobilization of sulphur in a soil during decomposition of plant residues of varied chemical composition and S content". *Plant and soil, 360*(1), 391-404.

O'Gorman, P. A. 2015. "Precipitation extremes under climate change". *Current Climate Change Reports, 1*(2), 49-59.

Ofiti, N. O. E., Zosso, C. U., Soong, J. L., et al. 2021. "Warming promotes loss of subsoil carbon through accelerated degradation of plant-derived organic matter". *Soil Biology and Biochemistry, 156*, 108185.

Penn, C. J., Bryant, R. B., Callahan, M. P., et al. 2011. "Use of industrial by-products to sorb and retain phosphorus". *Communications in Soil Science and Plant Analysis, 42*(6), 633-644.

Piutti, S., Slezack-Deschaumes, S., Niknahad-Gharmakher, H., et al. 2015. "Relationships between the density and activity of microbial communities possessing arylsulfatase activity and soil sulfate dynamics during the decomposition of plant residues in soil". *European Journal of Soil Biology, 70*, 88-96.

Prietzel, J., Botzaki, A., Tyufekchieva, N., et al. 2011. "Sulfur speciation in soil by S K-edge XANES spectroscopy: comparison of spectral deconvolution and linear combination fitting". *Environmental Science & Technology, 45*(7), 2878-2886.

Prietzel, J., Thieme, J., Salomé, M., et al. 2007. "Sulfur K-edge XANES spectroscopy reveals differences in sulfur speciation of bulk soils, humic acid, fulvic acid, and particle size separates". *Soil Biology and Biochemistry, 39*(4), 877-890.

Regnell, O., & Watras, C. J. 2019. "Microbial mercury methylation in aquatic environments: A critical review of published field and laboratory studies". *Environmental Science & Technology, 53*(1), 4-19.

Ritchie, H., & Roser, M. 2021. "Air Pollution". *Published Online at OurWorldInData.org. Available online: https://ourworldindata.org/explorers/air-pollution*.

Singh, B., Rengel, Z., & Bowden, J. W. 2006. "Carbon, nitrogen and sulphur cycling following incorporation of canola residue of different sizes into a nutrient-poor sandy soil". *Soil Biology and Biochemistry, 38*(1), 32-42.

Smolders, A., & Roelofs, J. G. M. 1993. "Sulphate-mediated iron limitation and eutrophication in aquatic ecosystems". *Aquatic Botany, 46*(3), 247-253.
Solomon, D., Lehmann, J., & Martínez, C. E. 2003. "Sulfur K-edge XANES spectroscopy as a tool for understanding sulfur dynamics in soil organic matter". *Soil Science Society of America Journal, 67*(6), 1721-1731.
Soong, J. L., & Cotrufo, M. F. 2015. "Annual burning of a tallgrass prairie inhibits C and N cycling in soil, increasing recalcitrant pyrogenic organic matter storage while reducing N availability". *Global Change Biology, 21*(6), 2321-2333.
Spohn, M. 2020. "Phosphorus and carbon in soil particle size fractions: A synthesis". *Biogeochemistry, 147*(3), 225-242.
Spohn, M. 2024. "Preferential adsorption of nitrogen- and phosphorus-containing organic compounds to minerals in soils: A review". *Soil Biology and Biochemistry, 194*, 109428.
Tanikawa, T., Hashimoto, Y., Yamaguchi, N., et al. 2014. "Sulfur accumulation in Melanudands during development by upbuilding pedogenesis since 14–15cal.ka". *Geoderma, 232-234*, 609-618.
Tanikawa, T., Noguchi, K., Nakanishi, K., et al. 2014. "Sequential transformation rates of soil organic sulfur fractions in two-step mineralization process". *Biology and Fertility of Soils, 50*(2), 225-237.
Tanikawa, T., Sase, H., Fukushima, S., et al. 2022. "Sulfur accumulation in soil in a forested watershed historically exposed to air pollution in central Japan". *Geoderma, 407*, 115544.
Tariq, A., Jensen, L. S., Sander, B. O., et al. 2018. "Paddy soil drainage influences residue carbon contribution to methane emissions". *Journal of Environmental Management, 225*, 168-176.
Tauchnitz, N., Bischoff, J., Schrödter, M., et al. 2018. "Nitrogen efficiency of strip-till combined with slurry band injection below the maize seeds". *Soil and Tillage Research, 181*, 11-18.
Tolu, J., Bouchet, S., Helfenstein, J., et al. 2022. "Understanding soil selenium accumulation and bioavailability through size resolved and elemental characterization of soil extracts". *Nature Communications, 13*(1), 6974.
Wang, F., & Chapman, P. M. 1999. "Biological implications of sulfide in sediment—a review focusing on sediment toxicity". *Environmental Toxicology and Chemistry, 18*(11), 2526-2532.
Wojdyr, M. 2010. "Fityk: a general-purpose peak fitting program". *Journal of Applied Crystallography, 43*(5 Part 1), 1126-1128.
Wright, A. L., & Hons, F. M. 2005. "Carbon and nitrogen sequestration and soil aggregation under sorghum cropping sequences". *Biology and Fertility of Soils, 41*(2), 95-100.
Yang, C., Lu, G., Chen, M., et al. 2016. "Spatial and temporal distributions of sulfur species in paddy soils affected by acid mine drainage in Dabaoshan sulfide mining area, South China". *Geoderma, 281*, 21-29.
Zeng, T., Arnold, W. A., & Toner, B. M. 2013. "Microscale characterization of sulfur speciation in lake sediments". *Environmental Science & Technology, 47*(3), 1287-1296.
Zheng, Y., Jin, J., Wang, X., et al. 2024. "Disentangling the effect of nitrogen supply on the priming of soil organic matter: A critical review". *Critical Reviews in Environmental Science and Technology, 54*(8), 676-697.
Zhu, M., Dam, T. T. N., Chadwick, O., et al. 2026. "Precipitation-driven shifts in organic sulfur decomposition and oxidation state along rainfall gradients". *Environmental Science & Technology*.

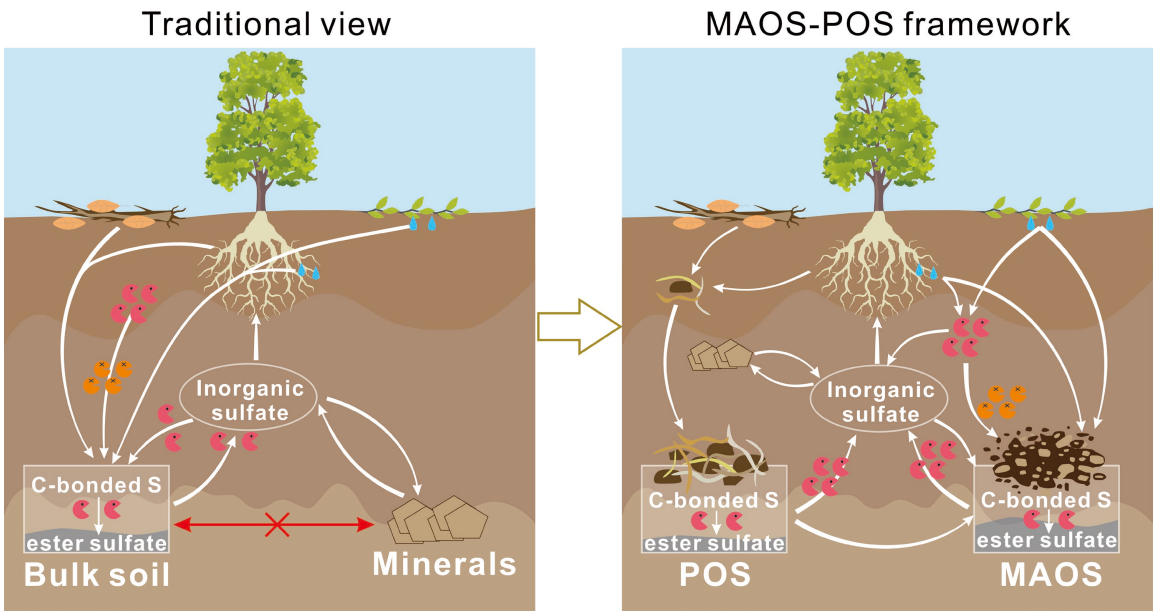

Figure 1. A two-pool conceptual framework for cycling of soil organic sulfur. Traditional research has treated organic-S mineralization at the bulk-soil scale, overlooking the stabilizing role of minerals. Here we separate organic S into particulate organic S (POS), largely derived from fragmented and translocated plant residues, and mineral-associated organic S (MAOS), formed through sorption of soluble compounds or by microbial transformation and subsequent deposition of microbial residues. Relative to POS, MAOS is typically more decomposed, chemically diverse, and sensitive to environmental change, yet its association with mineral surfaces constrains further conversion to plant-available sulfate. Ancillary pathways that influence inorganic sulfate are omitted for clarity.

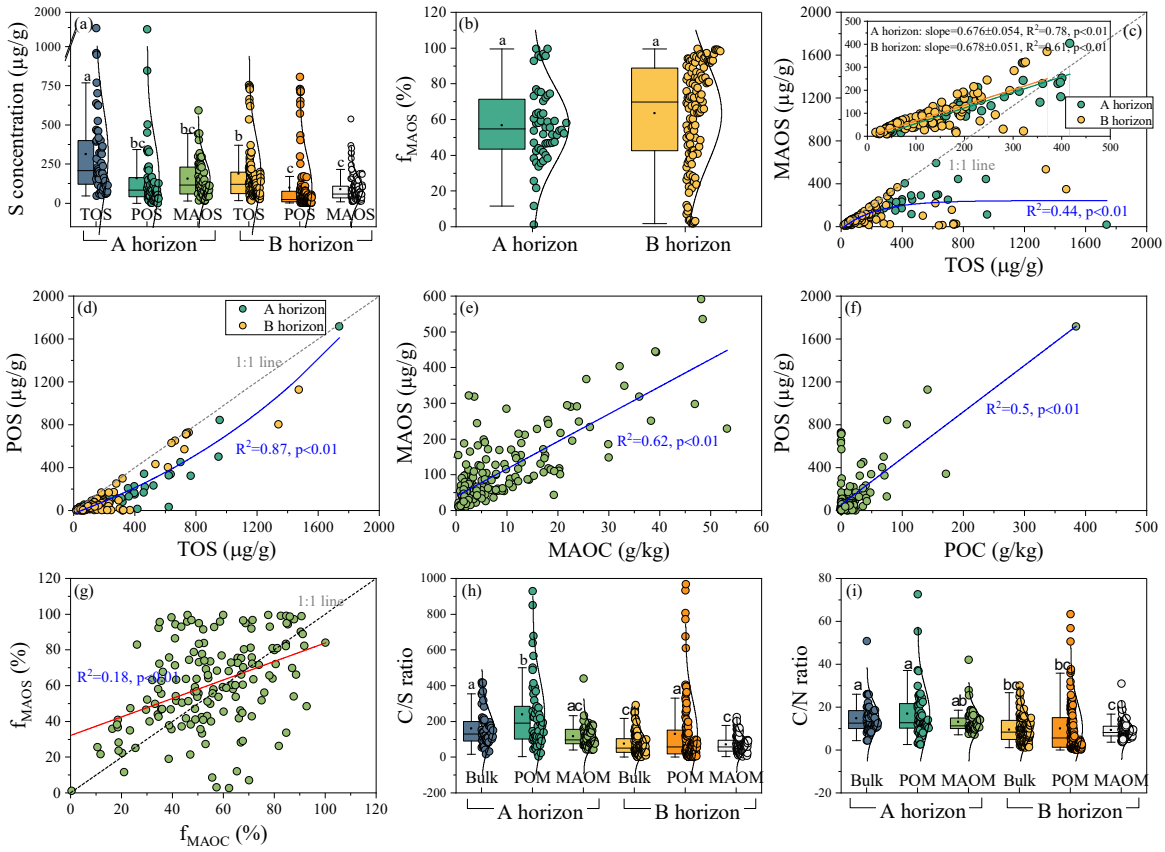

Figure 2. Distributions of MAOS and POS. (a) Distribution of organic S in bulk soil (TOS), POS and MAOS fractions in the A and B horizons. (b) Fractions of MAOS (f_{MAOS}) in the A and B horizons. (c, d) Correlations between TOS and MAOS or POS in concentrations in the A and B horizons. (e, f, g) Correlations between MAOS and MAOC, POS and POC, and f_{MAOS} and f_{MAOC}. (h, i) The C/S and C/N ratios in bulk soil, POM and MAOM fractions in the A and B horizons. POM is the sum of light POM and heavy POM. All concentrations are expresses as μg S /g bulk soils.

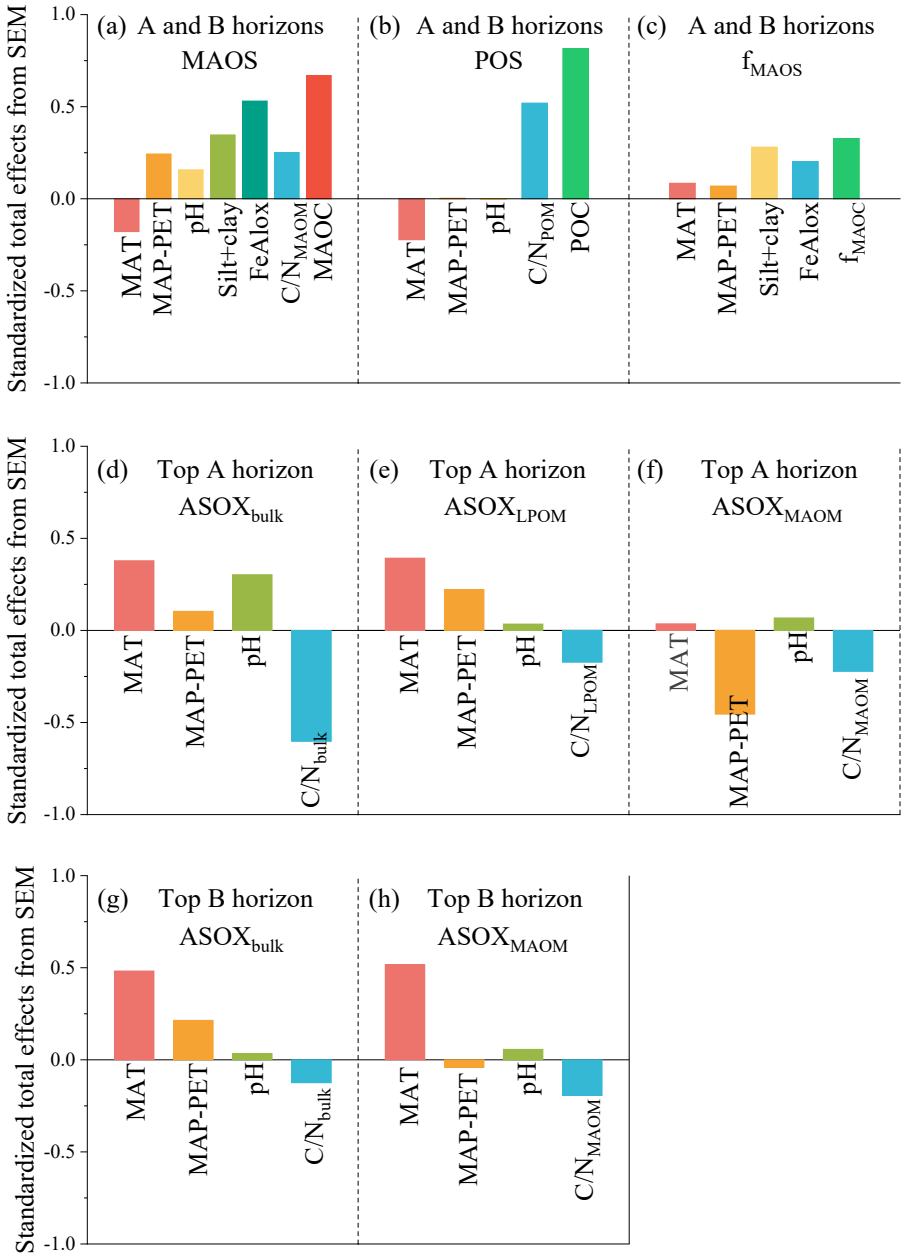

Figure 3. Standardized total effects (direct plus indirect effects) derived from the structural equation modelling. These effects show the controls on: (a-c) MAOS concentrations, POS concentrations, and f_{MAOS} in the A and B horizons; (d-f) average S oxidation states (ASOX) in bulk soil, LOPM and MAOM in the top A horizons; and (g, h) ASOX in bulk soil and MAOM in the top B horizons. The amount of LPOM material in B horizons was not sufficient for characterization.

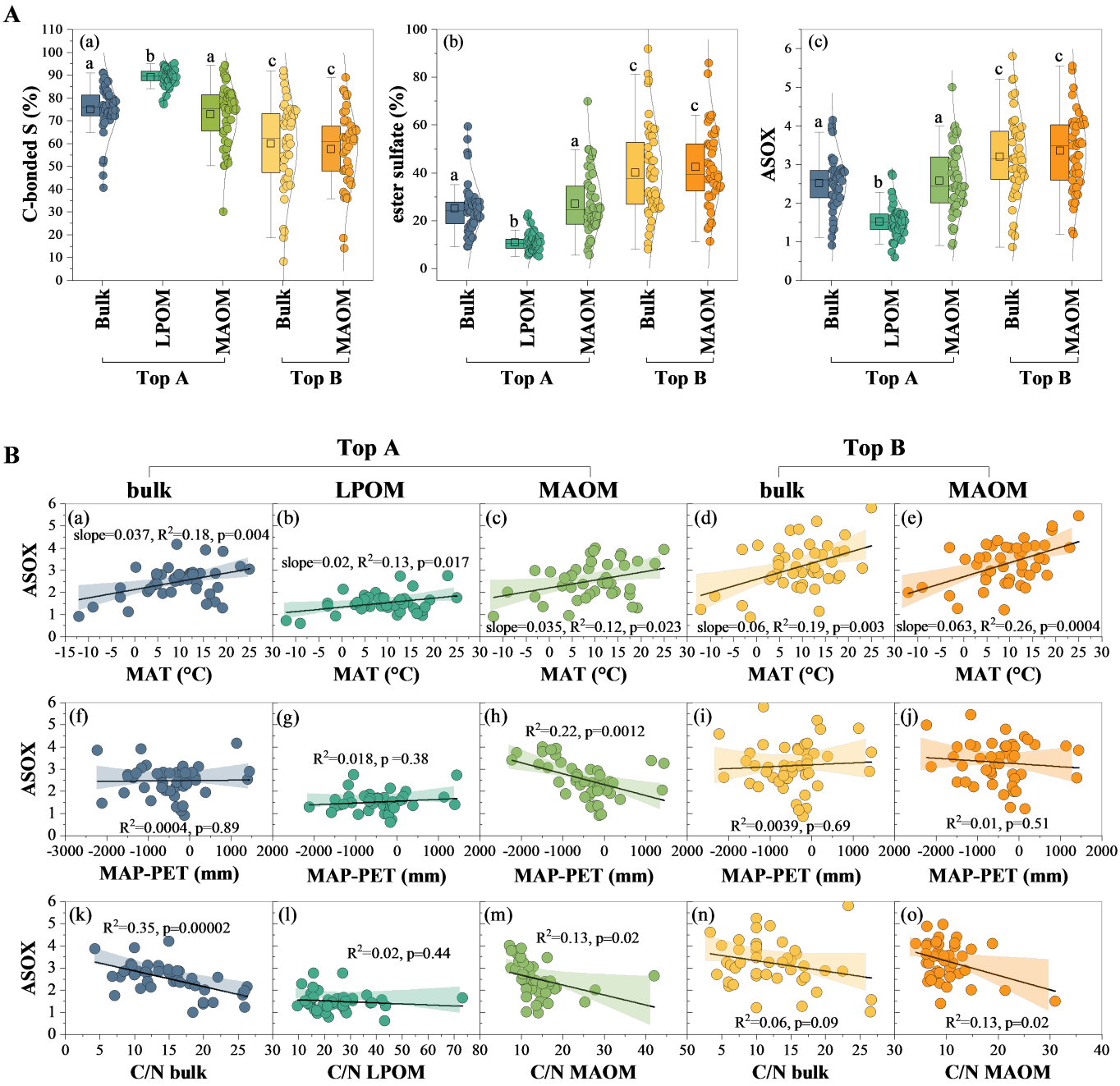

Figure 4. Chemical composition and oxidation states of MAOS and LPOS. (A) The chemical composition and average sulfur oxidation states (ASOX) in bulk soil, light particulate organic matter (LOPM) and mineral-associated organic matter (MAOM) in the top A and B horizons, and (B) their correlations with mean annual temperature (MAT), effective soil moisture (mean annual precipitation minus potential evapotranspiration, i.e., MAP-PET), and the C/N ratio.

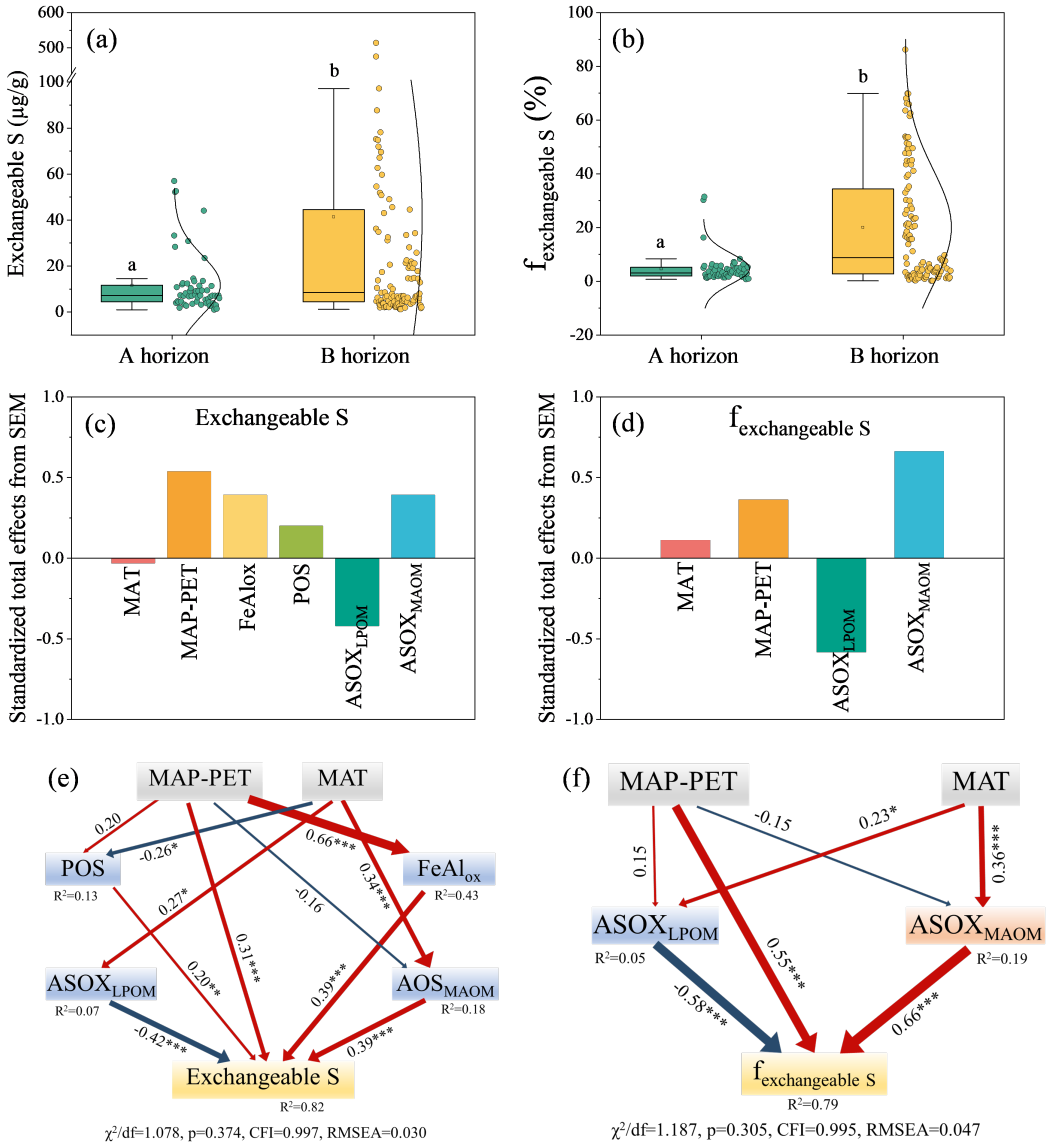

Figure 5. Sulfate availability and effects. (a, b) Concentration and proportion of exchangeable S in the A and B horizons. (c, d) Standardized total effects (direct plus indirect effects) derived from (e, f) the structural equation modelling (SEM) identifying the controls on exchangeable S concentration and percentage in the A and B horizons.

Supporting Information for

Mineral stabilization of soil organic sulfur at the continental scale

Zhuojun Zhang[1,2], M. Francesca Cotrufo[3], Benjamin L. Turner[4], Hai-Ruo Mao[1], Chao Liang[5], Mohsen Shakouri[6], and Mengqiang Zhu[1,7]*

[1] Department of Ecosystem Science and Management, University of Wyoming, Laramie, Wyoming 82071, United States

[2] State Key Laboratory of Lake and Watershed Science for Water Security, Nanjing Institute of Geography and Limnology, Chinese Academy of Sciences, Nanjing, Jiangsu 211135, China

[3] Department of Soil and Crop Science and Natural Resource Ecology Laboratory, Colorado State University, Fort Collins, Colorado 80523, United States

[4] Institute of Agriculture and Life Sciences, Gyeongsang National University, 501 Jinju-Daero, Jinju 52828, South Korea

[5] Institute of Applied Ecology, Chinese Academy of Sciences, Shenyang, Liaoning 110016, China

[6] Canadian Light Source Inc., University of Saskatchewan, Saskatoon, Saskatchewan S7N 2V3, Canada

[7] Department of geological, Environmental, and Planetary Sciences, University of Maryland, College Park, Maryland 20740, United States

* Corresponding author: Mengqiang Zhu

Email: mqzhu@umd.edu

This PDF file includes:

Figures S1 to S9
Tables S2

Other supporting materials for this manuscript include the following:

Table S1

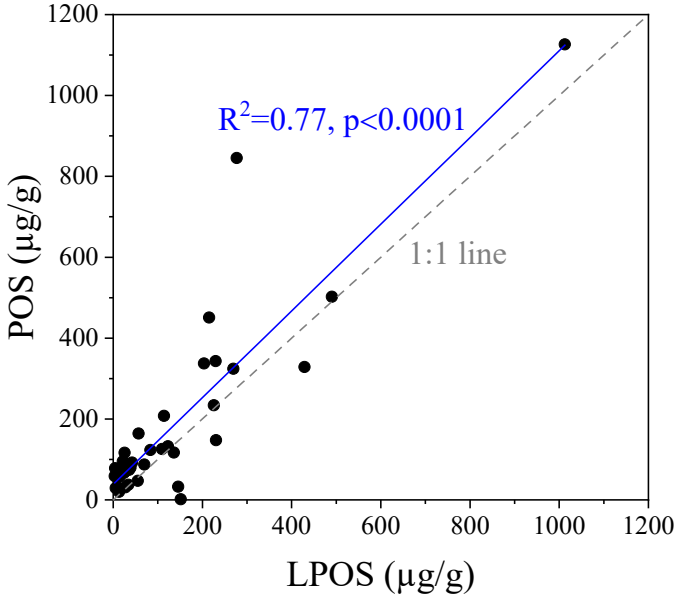

Fig. S1. Correlation between LPOS and POS in the topsoil.

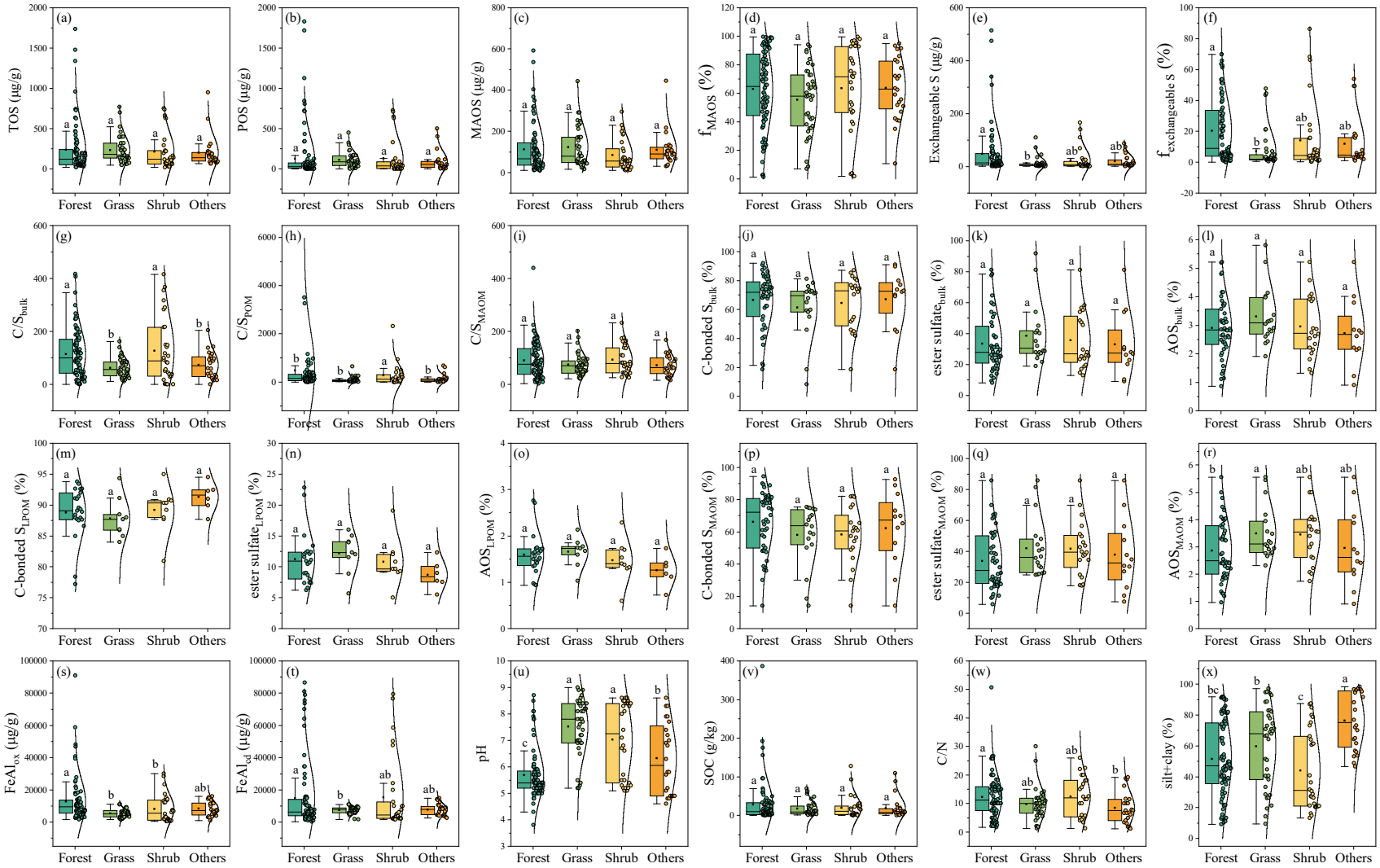

Fig. S2. A comparative analysis of key organic S and soil characteristics across different ecosystems.

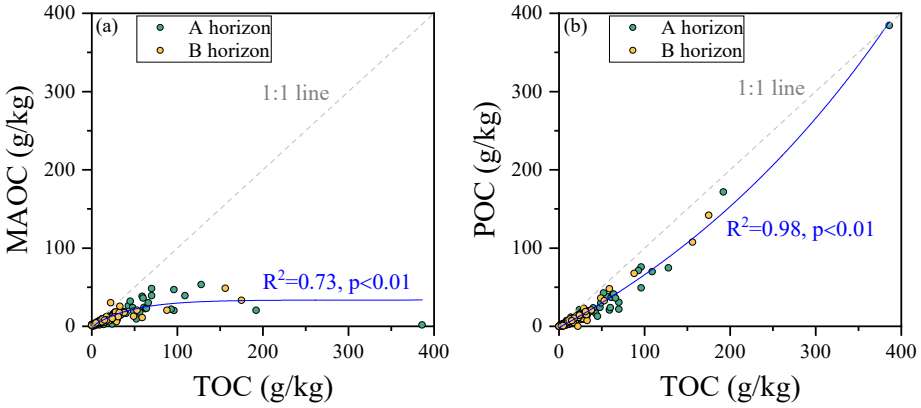

Fig. S3. Correlations between TOC (g/kg soil) and concentrations of MAOC and POC (g/kg soil) in the A and B horizons.

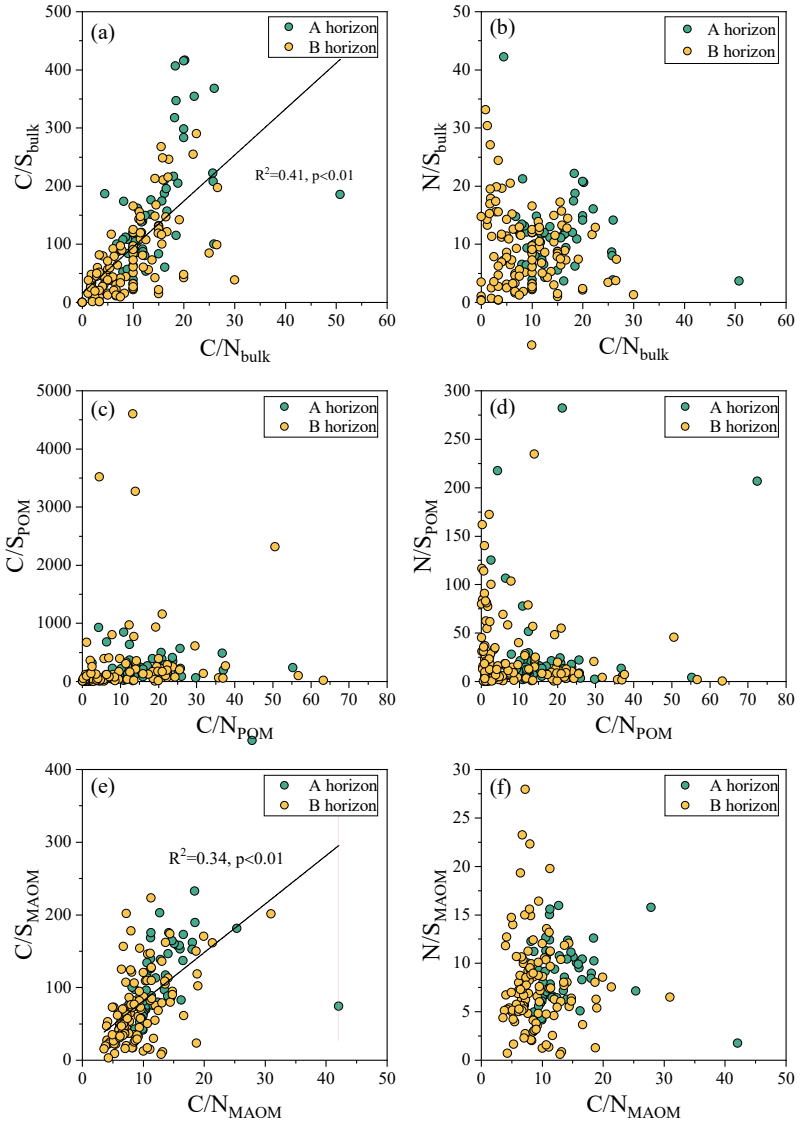

Fig. S4. Correlations between C/S and C/N ratios, as well as N/S and C/N ratios, in bulk soil, POM, and MAOM fractions.

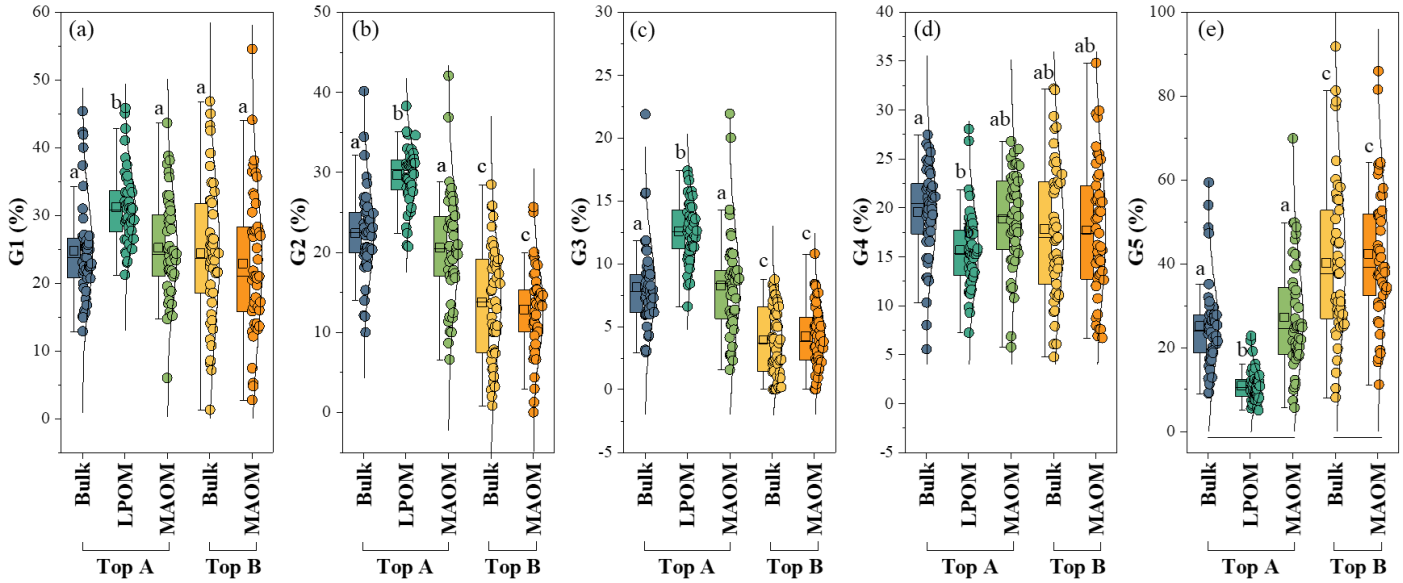

Fig. S5. The chemical composition of organic S groups in bulk soil, LOPM and MAOM in the top A and B horizons.

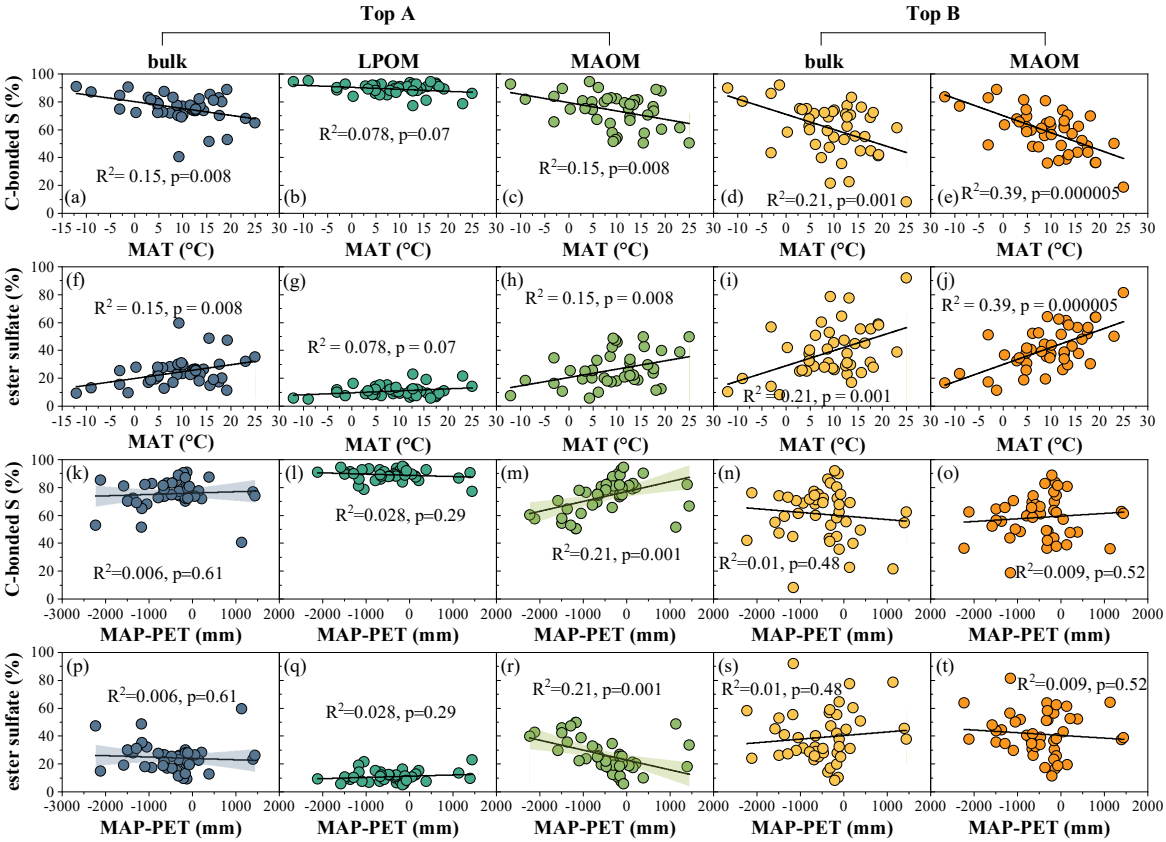

Fig. S6. Correlations of the proportions of C-bonded S and ester sulfate with MAT and MAP-PET in bulk soil, LOPM, and MAOM across the top A and B horizons.

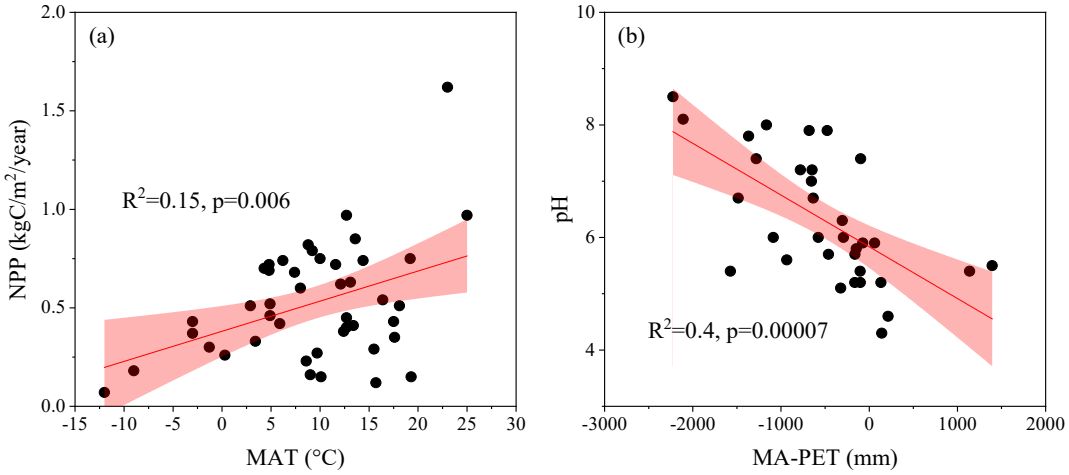

Fig. S7. (a) Correlation between NPP and MAT, and (b) correlation between soil pH and MAP-PET (b).

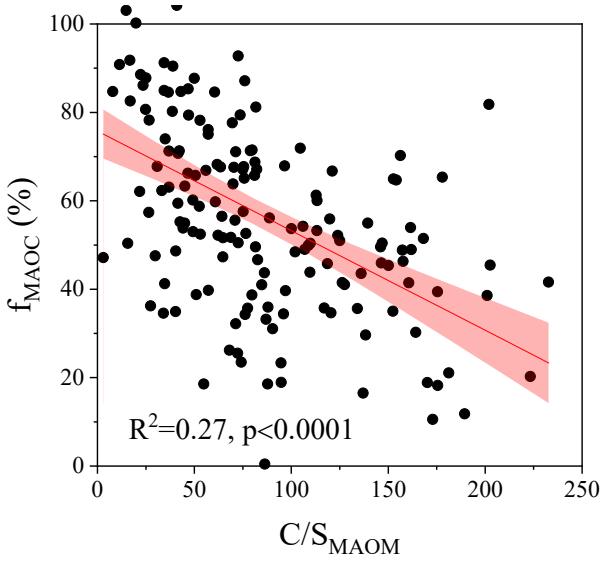

Fig. S8. Correlation between f_{MAOC} and C/S_{MAOM}.

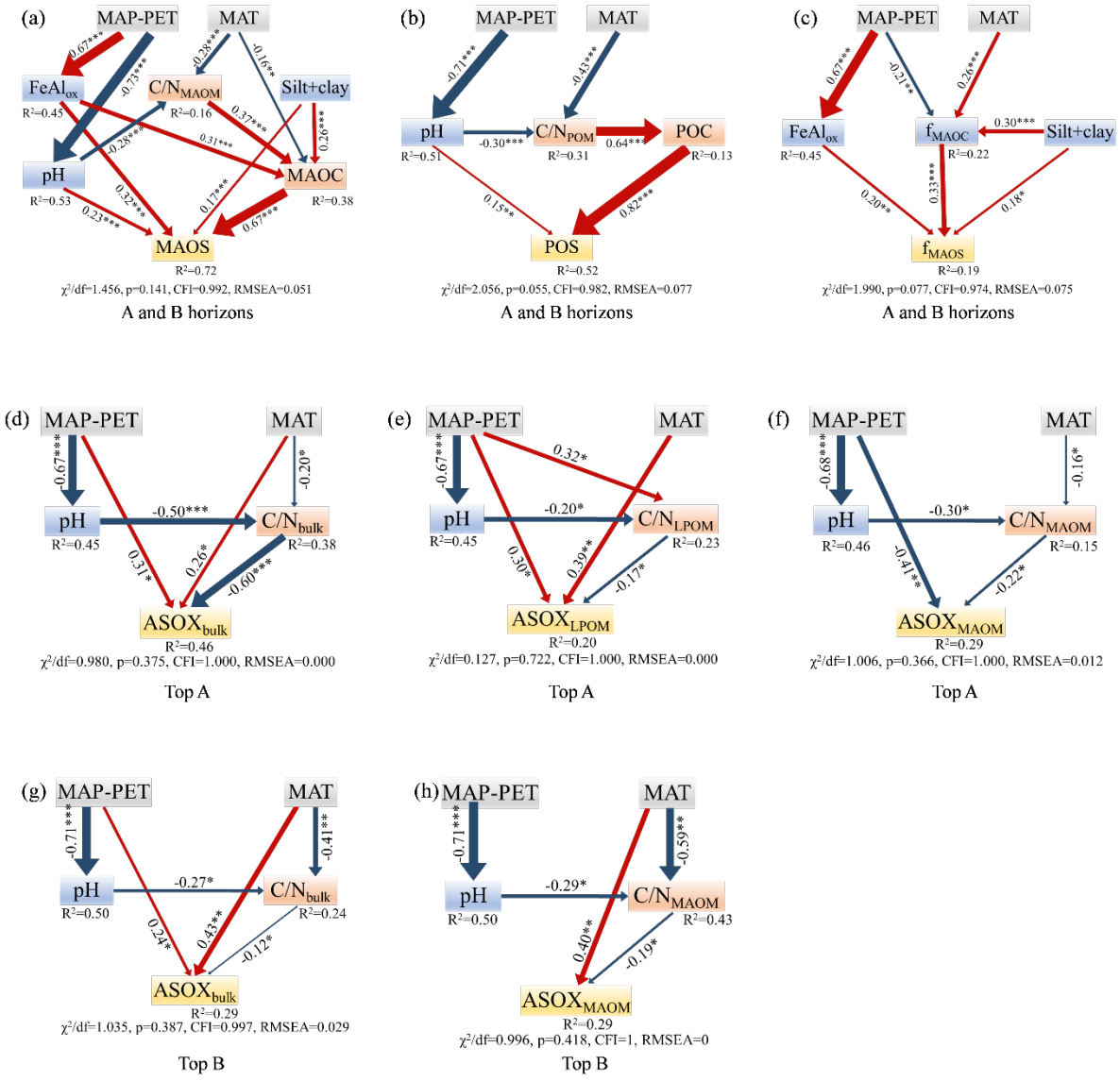

Fig. S9. A schematic representation of the structural equation modelling used to identify the controls on MAOS concentrations, POS concentrations, f_{MAOS} in the A and B horizons (a-c), ASOX in bulk soil, LOPM and MAOM in the top A horizons (d-f), and ASOX in bulk soil and MAOM in the top B horizons (g, h).

Table S2 The relative proportions of S species obtained from the Gaussian curve fitting results.

Sample name	G1 (%)	G2 (%)	G3 (%)	G4 (%)	G5 (%)	Average oxidation state
ABBY_A_bulk	23.0	23.6	8.2	21.9	23.3	2.5
BARR_Cgjj_bulk	45.4	26.8	8.5	10.3	9.0	0.9
BART_A_bulk	15.1	40.1	15.6	16.6	12.7	1.9
BLAN_Ap1_bulk	19.9	23.1	6.0	24.9	26.2	2.8
BONA_Bg Oajj_bulk	37.4	20.6	7.3	19.2	15.6	1.8
CLBJ_A_bulk	42.3	19.6	6.0	14.9	17.3	1.6
CPER_A_bulk	21.4	26.0	7.4	17.4	27.8	2.6
DCFS_A1_bulk	21.8	22.1	7.8	24.2	24.0	2.7
DEJU_A_bulk	31.0	20.3	9.2	14.3	25.2	2.2
DELA_A1_bulk	22.5	20.4	6.2	21.0	29.9	2.8
GRSM_A1_bulk	23.8	20.6	8.0	23.9	23.7	2.6
GUAN_A_bulk	19.3	18.1	6.0	24.7	32.0	3.2
HARV_A_bulk	15.9	22.5	6.9	26.5	28.2	3.1
HEAL_A Cjj_bulk	41.9	26.2	9.8	12.8	9.4	1.1
JERC_A_bulk	26.9	34.4	21.9	5.5	11.3	1.3
JORN_A_bulk	29.6	32.1	15.7	8.0	14.6	1.5
OAES_Klemme_A_bulk	15.6	12.1	3.1	20.6	48.5	3.9
KONA_AP_bulk	26.7	19.9	5.0	22.1	26.3	2.6
KONZ_A_bulk	21.9	20.6	6.0	24.9	26.6	2.8
LAJA_Ap_bulk	24.9	15.3	4.2	20.4	35.2	3.0
LENO_A_bulk	27.2	24.1	9.2	19.4	20.1	2.2
Mameyes_A_bulk	12.9	14.0	4.3	14.8	54.0	4.0
MLBS_A_bulk	23.8	25.0	6.3	22.5	22.5	2.5
MOAB_A_bulk	25.4	18.6	6.5	19.9	29.7	2.7
NIWO_A1_bulk	17.6	18.7	8.3	27.5	27.8	3.1
NOGP_A1_bulk	20.8	22.5	7.8	21.6	27.3	2.8
ONAQ_A1_bulk	25.3	19.9	7.4	17.3	30.0	2.7
ORNL_A_bulk	18.8	23.8	7.2	23.8	26.4	2.8
PUUM_Bw1_bulk	21.6	19.5	6.6	26.2	26.0	2.9
RMNP_A_bulk	26.2	26.8	11.8	18.3	16.8	2.0
SCBI_A_bulk	22.4	23.8	7.9	23.5	22.4	2.6
SERC_A_bulk	24.9	24.1	7.9	20.3	22.7	2.4
SJER_A1_bulk	34.3	20.5	9.7	16.6	18.9	1.9
SOAP_A1_bulk	22.3	29.4	11.9	18.6	17.8	2.2
SRER_A_bulk	16.7	12.0	3.0	21.0	47.2	3.8
STEI_A_bulk	25.5	22.8	8.9	22.0	20.8	2.4
STER_Ap1_bulk	25.0	18.2	6.0	19.9	30.9	2.8
TEAK_A_bulk	25.6	28.6	11.1	17.6	17.1	2.0
TOOL_Bg_bulk	40.0	25.1	9.2	12.9	12.9	1.3
TREE_A E_bulk	20.7	22.0	7.3	22.2	27.8	2.8
UKFS_A1_bulk	22.5	20.3	6.1	25.7	25.4	2.8

UNDE_A_bulk	22.9	25.7	11.0	21.2	19.2	2.3
WOOD_AO_bulk	25.9	23.1	8.2	21.1	21.6	2.4
WREF_Ac_bulk	15.0	10.0	3.1	12.5	59.4	4.2
YELL_A_bulk	27.0	24.9	10.2	19.3	18.7	2.1
ABBY_Bw1_bulk	37.2	6.5	1.4	9.4	45.5	2.9
BARR_CgjjF2_bulk	39.2	28.4	8.3	13.8	10.3	1.2
BART_Bs1_bulk	18.7	13.6	6.7	10.4	50.7	3.6
BLAN_Bt1_bulk	32.2	7.4	2.1	11.1	47.2	3.1
BONA_Cg_bulk	43.2	20.8	7.1	15.0	13.9	1.4
CLBJ_Bt1_bulk	32.2	15.2	2.2	19.1	31.3	2.6
CPER_Bt1_bulk	27.4	11.9	2.3	17.5	40.8	3.2
DCFS_Bw_bulk	22.5	15.3	3.6	26.6	32.1	3.2
DEJU_Bw_bulk	23.1	2.8	4.2	13.2	56.7	3.9
DELA_Bt_bulk	19.8	11.1	2.4	11.4	55.3	3.8
GRSM_Bw_bulk	8.2	2.0	0.0	12.2	77.6	5.2
GUAN_Bk1_bulk	23.5	18.0	3.2	16.6	38.8	3.1
HARV_Bw1_bulk	8.5	5.4	1.5	24.6	60.1	4.8
HEAL_Cfjj_bulk	46.8	25.7	8.4	10.9	8.1	0.9
JERC_Bt1_bulk	24.6	5.5	0.0	11.1	58.8	3.9
JORN_Bw_bulk	22.2	23.2	8.2	22.6	23.8	2.6
OAES_Klemme_Bw_bulk	15.4	10.0	2.6	16.7	55.2	4.1
KONA_Bt1_bulk	34.9	19.6	4.1	18.6	22.9	2.1
KONZ_Bt1_bulk	25.6	16.2	4.0	25.2	29.0	2.9
LAJA_Bssyz1_bulk	1.3	0.8	0.0	6.1	91.8	5.8
LENO_Bw_bulk	25.6	18.6	5.8	22.2	27.9	2.7
Mameyes_Bkk1_bulk	7.1	3.7	0.0	7.9	81.3	5.2
MLBS_Bg1_bulk	42.5	10.2	2.0	14.4	30.9	2.2
MOAB_Bw_bulk	31.8	19.2	5.0	18.0	26.0	2.3
NIWO_Bw1_bulk	11.6	10.7	3.7	32.2	41.8	4.1
NOGP_Bt1_bulk	30.2	18.0	7.9	15.3	28.6	2.4
ONAQ_Bw_bulk	23.7	7.8	1.0	14.7	52.8	3.7
ORNL_Bt1_bulk	23.4	7.5	0.5	23.8	44.9	3.7
PUUM_2Bw2_bulk	14.0	13.9	5.2	29.4	37.6	3.8
RMNP_AB_bulk	24.7	21.4	7.5	21.5	24.9	2.6
SCBI_Bt1_bulk	21.4	4.5	0.2	9.5	64.5	4.2
SERC_Bt1_bulk	45.0	24.5	7.5	6.1	16.9	1.1
SJER_Bw_bulk	26.6	10.0	1.4	17.0	45.0	3.4
SOAP_Bt1_bulk	21.6	20.8	6.1	21.9	29.5	2.9
SRER_Bw_bulk	10.8	7.3	0.9	22.7	58.3	4.6
STEI_Bs1_bulk	17.1	16.8	6.0	22.4	37.7	3.4
STER_Bt_bulk	34.8	18.8	5.0	14.5	27.0	2.2
TEAK_2C3_bulk	21.6	19.2	8.7	22.6	27.9	2.9
TOOL_Cg_bulk	33.5	25.8	7.2	13.8	19.7	1.8
TREE_Bs_bulk	18.5	17.3	7.0	24.7	32.5	3.2

UKFS_Bt1_bulk	25.8	12.9	2.3	28.1	30.9	3.1
UNDE_BS1_bulk	26.5	16.1	4.0	28.3	25.1	2.8
WOOD_2Bw_bulk	14.5	10.9	2.4	32.0	40.3	4.0
WREF_Bw_bulk	13.2	3.2	0.2	4.7	78.6	4.8
YELL_Bt1_bulk	24.4	20.0	6.6	23.4	25.6	2.7
ABBY_A_maom	27.7	26.4	9.1	18.7	18.1	2.1
BARR_Cgjj_maom	43.6	28.8	8.4	11.8	7.4	0.9
BART_A_maom	19.5	42.0	13.9	14.7	9.9	1.6
BLAN_Ap1_maom	25.0	23.1	9.4	21.0	21.6	2.4
BONA_Bg Oajj_maom	37.5	20.8	6.2	19.3	16.1	1.8
CLBJ_A_maom	38.8	17.8	7.5	12.2	23.7	1.9
CPER_A_maom	17.0	24.0	6.1	17.4	35.6	3.1
DCFS_A1_maom	23.0	18.9	8.3	25.1	24.6	2.8
DEJU_A_maom	21.9	17.1	9.0	17.6	34.4	3.0
DELA_A1_maom	33.0	23.5	2.7	13.9	26.9	2.2
GRSM_A1_maom	24.1	23.6	9.3	21.8	21.2	2.4
GUAN_A_maom	18.5	16.6	8.0	18.1	38.9	3.3
HARV_A_maom	22.0	27.4	9.2	21.3	20.2	2.4
HEAL_A Cjj_maom	36.4	27.8	10.5	14.7	10.6	1.4
JERC_A_maom	32.0	28.0	21.9	5.8	12.3	1.3
JORN_A_maom	17.5	11.3	4.1	24.4	42.7	3.7
Klemme_A_maom	23.3	8.6	2.7	15.7	49.7	3.6
KONA_AP_maom	30.2	19.5	5.2	14.6	30.6	2.5
KONZ_A_maom	25.1	19.1	7.8	23.1	25.0	2.7
LAJA_Ap_maom	15.7	11.9	2.8	19.8	49.8	3.9
LENO_A_maom	35.6	27.0	14.3	11.9	11.2	1.3
Mameyes_A_maom	6.0	6.6	1.6	15.9	69.9	5.0
MLBS_A_maom	32.9	22.8	8.6	18.3	17.3	1.9
MOAB_A_maom	15.1	10.1	3.4	25.7	45.8	4.0
NIWO_A1_maom	21.5	17.4	9.1	26.8	25.2	2.9
NOGP_A1_maom	21.8	17.8	6.3	21.4	32.6	3.0
ONAQ_A1_maom	14.7	13.5	5.1	24.5	42.2	3.8
ORNL_A_maom	29.1	25.4	9.2	17.7	18.5	2.0
PUUM_Bw1_maom	18.8	17.4	5.6	24.6	33.6	3.3
RMNP_A_maom	25.4	23.3	10.9	21.2	19.2	2.3
SCBI_A_maom	24.8	22.1	9.5	22.8	20.9	2.4
SERC_A_maom	31.4	24.5	8.7	16.6	18.9	1.9
SJER_A1_maom	16.9	16.8	10.8	26.0	29.5	3.2
SOAP_A1_maom	21.0	26.4	12.4	17.9	22.3	2.4
SRER_A_maom	24.8	10.0	2.3	23.3	39.6	3.4
STEI_A_maom	28.6	20.0	12.2	19.1	20.2	2.2
STER_Ap1_maom	15.1	11.8	5.4	20.5	47.1	3.9
TEAK_A_maom	38.1	19.8	8.8	15.3	17.8	1.7
TOOL_Bg_maom	29.4	24.5	10.1	17.5	18.4	2.0

TREE_A E_maom	21.4	20.5	10.8	22.1	25.2	2.7
UKFS_A1_maom	27.9	20.6	6.3	23.2	21.9	2.4
UNDE_A_maom	30.7	36.9	20.0	6.9	5.6	1.0
WOOD_AO_maom	23.8	19.8	6.3	24.3	25.8	2.7
WREF_Ac_maom	23.3	12.5	4.8	10.8	48.7	3.4
YELL_A_maom	24.3	20.9	7.2	22.7	24.9	2.6
ABBY_Bw1_maom	36.5	11.0	3.3	12.0	37.2	2.6
BARR_CgjjF2_maom	30.4	25.0	7.3	20.8	16.5	2.0
BART_Bs1_maom	12.8	11.3	5.0	18.8	52.0	4.1
BLAN_Bt1_maom	20.4	11.3	2.4	14.4	51.4	3.7
BONA_Cg_maom	37.5	19.5	6.7	19.0	17.4	1.8
CLBJ_Bt1_maom	21.8	12.5	5.1	8.7	51.8	3.5
CPER_Bt1_maom	27.6	12.0	3.4	12.7	44.3	3.1
DCFS_Bw_maom	26.8	17.3	4.5	20.8	30.7	2.8
DEJU_Bw_maom	12.1	13.8	5.0	17.9	51.2	4.0
DELA_Bt_maom	13.9	12.2	2.3	15.5	56.2	4.1
GRSM_Bw_maom	7.5	13.5	3.0	14.7	61.3	4.5
GUAN_Bk1_maom	15.8	10.3	2.4	21.3	50.1	4.0
HARV_Bw1_maom	13.5	6.7	2.6	24.5	52.6	4.3
HEAL_Cfjj_maom	44.1	19.4	10.8	14.6	11.2	1.3
JERC_Bt1_maom	14.0	0.0	0.0	22.3	63.7	4.8
JORN_Bw_maom	27.8	10.6	4.3	19.6	37.7	3.1
Klemme_Bw_maom	16.4	10.0	1.1	16.2	56.3	4.1
KONA_Bt1_maom	27.9	15.2	3.9	15.7	37.5	2.9
KONZ_Bt1_maom	33.3	17.4	5.7	17.4	26.2	2.3
LAJA_Bssyz1_maom	5.2	1.3	0.0	12.0	81.5	5.4
LENO_Bw_maom	25.2	18.6	6.5	19.6	30.2	2.8
Mameyes_Bkk1_maom	2.7	2.9	0.4	8.0	85.9	5.6
MLBS_Bg1_maom	54.6	14.6	2.4	9.1	19.4	1.2
MOAB_Bw_maom	17.1	8.0	1.8	29.6	43.5	4.0
NIWO_Bw1_maom	17.9	14.4	5.5	25.5	36.6	3.5
NOGP_Bt1_maom	28.3	14.4	3.6	13.1	40.5	2.9
ONAQ_Bw_maom	32.9	16.3	8.4	6.9	35.6	2.4
ORNL_Bt1_maom	31.8	15.4	2.2	7.6	43.1	2.8
PUUM_2Bw2_maom	13.2	13.3	5.4	29.2	38.9	3.8
RMNP_AB_maom	19.7	15.3	6.9	25.5	32.5	3.2
SCBI_Bt1_maom	21.0	6.9	2.2	7.6	62.3	4.0
SERC_Bt1_maom	21.0	4.3	3.3	13.3	58.1	4.0
SJER_Bw_maom	20.7	9.6	8.3	13.5	47.9	3.6
SOAP_Bt1_maom	38.1	14.8	4.7	12.6	29.7	2.2
SRER_Bw_maom	4.8	7.4	0.9	23.1	63.7	5.0
STEI_Bs1_maom	27.5	18.4	7.7	20.5	25.9	2.5
STER_Bt_maom	36.3	14.1	4.2	10.7	34.7	2.4
TEAK_2C3_maom	16.4	14.9	6.1	23.4	39.2	3.6

TOOL_Cg_maom	27.0	25.6	8.2	16.0	23.2	2.2
TREE_Bs_maom	16.0	13.4	7.7	25.0	38.0	3.6
UKFS_Bt1_maom	23.5	13.3	3.3	26.2	33.7	3.2
UNDE_BS1_maom	35.7	20.0	5.0	20.6	18.6	2.0
WOOD_2Bw_maom	13.6	8.5	1.5	34.8	41.5	4.2
WREF_Bw_maom	21.0	6.6	1.6	6.7	64.1	4.0
YELL_Bt1_maom	17.2	14.6	3.8	30.0	34.4	3.5
ABBY_A LPOM	32.0	31.1	12.6	14.7	9.6	1.4
BARR_Cgjj/Oajj_LPOM	45.1	29.3	10.3	9.9	5.5	0.7
BART_A LPOM	26.4	38.3	14.1	13.8	7.4	1.3
BLAN_Ap1_LPOM	36.4	30.8	17.4	9.3	6.2	1.0
BONA_Bg Oajj LPOM	38.5	23.1	9.0	17.8	11.6	1.5
CLBJ_A_LPOM	41.0	28.1	12.9	11.4	6.6	1.0
CPER_A_LPOM	33.4	29.2	13.2	15.3	8.9	1.4
DCFS_A1_LPOM	29.0	27.3	10.6	19.0	14.0	1.8
DEJU_A_LPOM	29.4	33.0	15.7	12.2	9.7	1.4
DELA_A1_LPOM	31.5	34.7	14.8	11.3	7.7	1.2
GRSM_A1_LPOM	31.0	29.1	10.8	17.0	12.1	1.6
GUAN_A LPOM	21.2	20.8	8.3	28.0	21.6	2.8
HARV_A_LPOM	24.5	30.9	9.8	19.7	15.0	2.0
HEAL_A/Cjj_LPOM	42.8	27.5	11.1	11.2	7.4	0.9
JERC_A_LPOM	24.3	34.7	14.7	15.3	10.9	1.6
JORN_A LPOM	35.6	26.6	15.4	13.2	9.1	1.3
Klemme_A_LPOM	26.5	22.4	10.2	21.8	19.1	2.3
KONA_AP_LPOM	37.4	28.8	13.8	12.5	7.5	1.1
KONZ_A_LPOM	29.4	30.8	12.2	16.0	11.5	1.6
LAJA_Ap_LPOM	33.4	24.5	9.6	18.5	14.0	1.7
LENO_A_LPOM	31.8	32.4	12.7	14.1	9.0	1.3
Mameyes_A_LPOM	29.7	28.2	11.4	18.4	12.3	1.7
MLBS_A_LPOM	28.2	31.9	8.4	19.0	12.5	1.7
MOAB_A_LPOM	34.9	28.3	13.6	13.9	9.3	1.3
NIWO_A1_LPOM	25.7	25.0	12.0	21.2	16.0	2.1
NOGP_A1_LPOM	27.4	30.8	11.6	15.1	15.1	1.8
ONAQ_A1_LPOM	31.9	25.6	13.7	18.4	10.4	1.6
ORNL_A_LPOM	29.1	31.2	13.0	16.0	10.7	1.6
PUUM_Bw1 LPOM	23.1	20.7	6.6	26.8	22.8	2.7
RMNP_A_LPOM	28.9	32.9	14.5	14.9	8.9	1.4
SCBI_A_LPOM	31.1	31.4	13.3	15.3	9.0	1.4
SERC_A_LPOM	27.7	30.9	11.9	17.4	12.1	1.7
SJER_A1_LPOM	35.8	31.1	15.8	11.6	5.7	1.0
SOAP_A1_LPOM	25.0	35.0	17.0	15.6	7.3	1.5
SRER						
STEI_A_LPOM	29.5	32.3	16.6	12.9	8.6	1.4
STER_Ap1_LPOM	34.0	28.4	12.2	15.3	10.1	1.4

TEAK_A_LPOM	26.5	31.7	13.6	16.3	12.0	1.7
TOOL_Bg_LPOM	45.8	29.9	12.1	7.2	5.0	0.6
TREE_A/E_LPOM	30.8	31.1	11.4	15.6	11.1	1.5
UKFS_A1_LPOM	31.1	27.5	11.4	17.6	12.4	1.7
UNDE_A_LPOM	33.4	31.2	14.5	12.9	8.0	1.2
WOOD_AO_LPOM	29.3	30.0	11.3	17.4	12.0	1.7
WREF_Ac LPOM	23.1	34.6	15.4	13.4	13.4	1.7
YELL_A_LPOM	31.0	29.7	12.6	15.8	10.8	1.5

Table S1 Detailed soil profile descriptions for the NEON sites

	domain	site abbr.	siteName	horizon	depth (cm)	Depth (cm)	unique ID	MAP-PET	MAT	NPP	silt_clay (%)	pH_H2O	Feox	Alox	Fecd	Alcd	Feoxcd	Aloxcd	TS	TOS	Exchangeable S	SOC	% MAOM of bulk soil mass	MAOS	POS	f_{MAOS}	OC in MAOM	N in MAOM	S in MAOM	OC in POM	N in POM	S in POM
								mm	°C	kgC/m2/year			ug/g soil	ug/g soil	ug/g soil	ug/g soil	ug/g soil	ug/g soil	ug/g soil	ug/g soil	ug/g soil	g/kg soil	%	ug/g soil	ug/g soil	%	g/kg	g/kg	ug/g	g/kg	g/kg	ug/g
NonOPM1	D01	HARV	Harvard Forest	A	4 -- 9	6.5	2	215	7.4	0.68	41	4.6	10942	7235	3896	870	14839	8105	669	636	33	96	42	298	337	47	113	7	716	164	12	578
NonOPM2	D01	HARV	Harvard Forest	Ap	9 -- 17	13	3	215	7.4	0.68	40	4.8	9959	7445	3490	761	13449	8206	496	468	28	59	45	251	217	54	85	5	559	106	7	393
NonOPM3	D01	HARV	Harvard Forest	Bw/E	17 -- 32	24.5	4	215	7.4	0.68	36	4.9	11089	13988	3826	901	14915	14889	299	224	75	33	40	155	69	69	44	3	389	55	3	115
NonOPM4	D01	HARV	Harvard Forest	Bw1	32 -- 53	42.5	5	215	7.4	0.68	30	5.0	7419	9795	2570	503	9988	10297	235	123	112	11	32	84	39	68	20	2	261	16	2	58
NonOPM5	D01	HARV	Harvard Forest	Bw2	53 -- 82	67.5	6	215	7.4	0.68	13	5.2	5356	4656	1263	284	6619	4939	110	74	36	3	13	37	37	50	12	1	274	3	0	43
NonOPM6	D10	CPER	Central Plains Experimental Ra	A	0 -- 10	5	15	-1368	8.6	0.23	29	7.8	1340	1006	5044	493	6384	1499	157	153	4	8	32	59	95	38	12	2	183	12	1	140
NonOPM7	D10	CPER	Central Plains Experimental Ra	BA	10 -- 30	20	16	-1368	8.6	0.23	26	6.9	2262	1121	4710	505	6973	1625	140	136	5	6	26	45	91	33	12	2	174	8	1	122
NonOPM8	D10	CPER	Central Plains Experimental Ra	Bt1	30 -- 54	42	17	-1368	8.6	0.23	34	7.5	1312	1444	4873	638	6185	2082	118	108	10	4	31	49	59	45	8	1	158	6	1	86
NonOPM9	D10	CPER	Central Plains Experimental Ra	Bt2	54 -- 81	67.5	18	-1368	8.6	0.23	51	8.1	959	1673	4193	687	5152	2360	95	89	6	4	45	67	22	76	6	1	149	7	2	40
NonOPM10	D10	CPER	Central Plains Experimental Ra	Bk1	81 -- 137	109	19	-1368	8.6	0.23	40	8.4	674	956	3911	358	4584	1313	65	52	14	2	56	47	5	90	3	0	83	5	1	12
NonOPM11	D10	CPER	Central Plains Experimental Ra	Bk2	137 -- 181	159	20	-1368	8.6	0.23	41	8.4	1081	746	4374	442	5455	1188	80	45	35	1	42	43	3	94	3	1	102	2	0	5
NonOPM12	D09	DCFS	Dakota Coteau Field School	A1	0 -- 8	4	22	-655	4.9	0.52	71	7.0	3279	1851	5908	1604	9186	3455	778	767	11	70	64	443	324	58	62	5	695	192	16	892
NonOPM13	D09	DCFS	Dakota Coteau Field School	A2	8 -- 18	13	23	-655	4.9	0.52	66	7.0	3986	2504	8152	1398	12138	3902	397	393	5	25	61	228	164	58	26	2	372	64	6	426
NonOPM14	D09	DCFS	Dakota Coteau Field School	A3	18 -- 26	22	24	-655	4.9	0.52	67	7.0	4182	2146	7835	1122	12017	3268	286	282	4	16	65	170	112	60	17	2	263	45	5	318
NonOPM15	D09	DCFS	Dakota Coteau Field School	Bw	26 -- 35	30.5	25	-655	4.9	0.52	64	7.6	4054	1596	6721	1112	10775	2708	239	235	4	19	64	155	80	66	20	2	242	53	4	223
NonOPM16	D09	DCFS	Dakota Coteau Field School	Bk1	35 -- 55	45	26	-655	4.9	0.52	69	8.3	1361	742	8063	854	9425	1596	143	140	3	9	77	36	103	26	10	1	47	39	6	450
NonOPM17	D09	DCFS	Dakota Coteau Field School	Bk2	55 -- 92	73.5	27	-655	4.9	0.52	68	8.5	1481	673	7735	674	9216	1347	323	321	2	5	76	22	299	7	5	1	30	20	2	1234
NonOPM18	D09	DCFS	Dakota Coteau Field School	BC	92 -- 110	101	28	-655	4.9	0.52	73	8.9	1779	671	8063	581	9842	1252	173	170	3	4	76	48	122	28	4	1	63	17	2	506
NonOPM19	D03	JERC	Jones Ecological Research Cen	A	0 -- 8	4	32	-323	19.2	0.75	14	5.7	1234	1304	1129	291	2363	1594	49	47	2	14	11	17	30	36	22	1	159	16	1	34
NonOPM20	D03	JERC	Jones Ecological Research Cen	E	8 -- 68	38	33	-323	19.2	0.75	16	5.4	1333	1468	1667	511	3000	1980	30	25	5	3	11	10	15	41	5	0	90	3	0	17
NonOPM21	D03	JERC	Jones Ecological Research Cen	Bt1	68 -- 105	86.5	34	-323	19.2	0.75	19	5.5	1745	1567	3094	672	4839	2238	32	23	8	1	17	14	9	60	4	1	82	1	0	11
NonOPM22	D03	JERC	Jones Ecological Research Cen	Bt2	105 -- 185	145	35	-323	19.2	0.75	24	5.4	2282	1760	6003	1177	8284	2937	39	21	17	1	17	12	9	56	3	0	69	1	0	11
NonOPM24	D09	WOOD	Woodworth	AO	0 -- 6	3	37	-647	4.9	0.46	45	7.2	3486	1609	5712	1009	9197	2618	408	401	7	56	39	253	148	63	46	4	652	91	8	241
NonOPM25	D09	WOOD	Woodworth	Ap	6 -- 16	11	38	-647	4.9	0.46	41	7.8	3906	1759	6170	954	10076	2713	232	227	5	24	41	211	16	93	33	3	520	40	4	28
NonOPM26	D09	WOOD	Woodworth	2Bw	16 -- 32	24	39	-647	4.9	0.46	26	8.1	3574	1284	10077	761	13651	2045	196	192	4	16	27	88	104	46	40	5	327	22	2	142
NonOPM27	D09	WOOD	Woodworth	2Bk1	32 -- 58	45	40	-647	4.9	0.46	14	8.5	4009	608	10362	465	14371	1073	186	182	4	6	17	22	160	12	23	3	129	7	1	193
NonOPM28	D09	WOOD	Woodworth	2Bk2	58 -- 92	75	41	-647	4.9	0.46	10	8.6	2796	350	8272	261	11069	610	187	183	4	2	13	16	168	9	9	1	120	2	0	193
NonOPM29	D02	BLAN	Blandy Experimental Farm	Ap1	2 -- 14	8	45	-292	12.1	0.62	74	6.0	5013	1925	21248	2360	26261	4285	223	212	12	18	78	155	57	73	15	1	199	80	8	255
NonOPM30	D02	BLAN	Blandy Experimental Farm	Ap2	14 -- 23	18.5	46	-292	12.1	0.62	74	5.8	5111	2028	24717	2625	29827	4653	199	187	13	10	79	143	43	77	8	1	181	47	4	207
NonOPM31	D02	BLAN	Blandy Experimental Farm	Bt1	23 -- 51	37	47	-292	12.1	0.62	82	6.1	4102	2243	30971	3446	35073	5689	243	200	43	3	82	165	36	82	3	0	200	17	1	200
NonOPM32	D02	BLAN	Blandy Experimental Farm	Bt2	51 -- 84	67.5	48	-292	12.1	0.62	81	6.6	3416	2216	37450	3898	40866	6114	254	199	55	1	93	187	12	94	2	0	200	15	8	187
NonOPM33	D10	STER	North Sterling, CO	Ap1	0 -- 11	5.5	60	-1280	9.7	0.27	53	7.4	1695	1348	3909	639	5604	1988	223	216	7	13	61	128	88	59	13	1	209	33	2	228
NonOPM34	D10	STER	North Sterling, CO	Ap2	11 -- 28	19.5	61	-1280	9.7	0.27	57	6.9	2038	1514	4027	695	6064	2209	206	203	3	8	61	105	98	52	10	1	173	20	2	248
NonOPM35	D10	STER	North Sterling, CO	Bt	28 -- 70	49	62	-1280	9.7	0.27	64	7.9	1257	1589	4235	622	5492	2211	197	195	2	6	69	105	90	54	8	1	153	19	3	287
NonOPM36	D10	STER	North Sterling, CO	Btk	70 -- 121	95.5	63	-1280	9.7	0.27	56	8.6	226	744	3589	408	3815	1152	289	280	9	0	63	30	250	11	3	1	48	0	1	681
NonOPM37	D11	OAES	Klemme Range Research Stati	A	0 -- 8	4	66	-1165	15.5	0.29	87	8.0	404	1535	19600	352	20003	1886	201	193	8	18	96	146	47	76	12	1	153	409	41	1078
NonOPM38	D11	OAES	Klemme Range Research Stati	Bw	8 -- 20	14	67	-1165	15.5	0.29	88	8.3	157	1649	23687	389	23844	2038	300	294	6	15	100	198	94	68	5	1	199	229	22	92799
NonOPM39	D14	JORN	Jornada LTER	A	0 -- 18	9	70	-2109	15.7	0.12	13	8.1	4002	1056	1788	335	5790	1391	120	117	3	2	17	39	78	34	10	1	231	2	0	94
NonOPM40	D14	JORN	Jornada LTER	Bw	18 -- 46	32	71	-2109	15.7	0.12	16	8.4	2474	920	2149	274	4623	1194	755	753	2	1	15	25	727	3	7	1	168	1	0	857
NonOPM41	D14	JORN	Jornada LTER	2Bk	46 -- 78	62	72	-2109	15.7	0.12	21	8.4	2084	927	2333	344	4418	1271	738	736	2	1	23	28	708	4	5	1	120	1	0	919
NonOPM42	D14	JORN	Jornada LTER	2Bkkm	78 -- 110	94	73	-2109	15.7	0.12	27	8.6	210	280	2003	222	2213	502	671	664	7	0	36	13	651	2	4	0	37	2	0	1012
NonOPM43	D14	JORN	Jornada LTER	2Bkk1	110 -- 173	141.5	74	-2109	15.7	0.12	32	8.4	211	221	1518	175	1729	396	671	640	31	0	44	11	628	2	4	0	26	1	0	1124
NonOPM44	D14	JORN	Jornada LTER	2Bkk2	173 -- 200	186.5	75	-2109	15.7	0.12	15	8.3	205	344	1501	156	1706	499	127	18	110	1	26	16	1	93	5	0	63	1	0	2
NonOPM45	D08	DELA	Dead Lake	A1	2 -- 15	8.5	76	-161	17.6	0.35	97	5.7	11447	2955	12467	1574	23914	4530	215	202	12	28	91	86	117	42	16	1	94	324	28	1355
NonOPM46	D08	DELA	Dead Lake	A2	15 -- 27	21	77	-161	17.6	0.35	88	5.1	11371	3934	11751	1879	23122	5813	190	159	31	19	91	89	71	56	12	1	97	229	23	854
NonOPM47	D08	DELA	Dead Lake	Bt1	27 -- 58	42.5	78	-161	17.6	0.35	77	4.6	11347	3573	9352	1337	20698	4910	176	143	32	6	79	73	70	51	4	1	93	28	4	326
NonOPM48	D08	DELA	Dead Lake	Bt2	58 -- 79	68.5	79	-161	17.6	0.35	72	4.8	8625	2602	9206	1130	17831	3733	178	90	88	2	73	65	25	72	2	0	89	7	1	93
NonOPM49	D08	DELA	Dead Lake	Bt3	79 -- 150	114.5	80	-161	17.6	0.35	73	4.8	7506	2482	13374	1461	20880	3943	127	65	63	1	70	60	4	93	2	0	86	3	1	15
NonOPM50	D08	DELA	Dead Lake	Bt4	150 -- 200	175	81	-161	17.6	0.35	70	4.9	5592	2164	11085	1404	16677	3568	139	64	75	1	72	58	6	91	2	0	81	4	1	21
NonOPM51	D02	SCBI	Smithsonian Conservation Biol	A	2 -- 7	4.5	82	-97	11.6	0.72	84	7.4	7347	2975	65327	4839	72674	7813	326	320	7	60	89	318	2	99	40	4	356	556	34	15
NonOPM52	D02	SCBI	Smithsonian Conservation Biol	BA	7 -- 14	10.5	83	-97	11.6	0.72	83	7.2	6385	3093	70186	5296	76571	8389	200	195	5	28	87	118	78	60	21	2	135	210	19	586
NonOPM53	D02	SCBI	Smithsonian Conservation Biol	Bt1	14 -- 34	24	84	-97	11.6	0.72	83	5.7	6557	3222	68196	5454	74753	8676	179	177	2	6	93	127	50	72	5	1	137	83	11	705
NonOPM54	D02	SCBI	Smithsonian Conservation Biol	Bt2	34 -- 59	46.5	85	-97	11.6	0.72	85	5.4	7724	3091	59408	4622	67132	7714	258	120	138	2	92	101	19	84	2	0	109	26	5	252
NonOPM55	D02	SCBI	Smithsonian Conservation Biol	Bt3	59 -- 114	86.5	86	-97	11.6	0.72	82	5.5	6241	2427	73550	5314	79791	7741	224	109	115	1	86	97	12	89	2	0	113	7	2	84
NonOPM56	D02	SCBI	Smithsonian Conservation Biol	2Bt4	114 -- 146	130	87	-97	11.6	0.72	86	5.4	8681	2598	76890	4038	85571	6636	162	113	49	1	96	91	22	80	1	0	95	24	10	536
NonOPM57	D02	SCBI	Smithsonian Conservation Biol	2Bt5	146 -- 179	162.5	88	-97	11.6	0.72	90	5.6	7809	1916	81502	5007	89311	6924	101	81	21	1	97	70	11	86	1	0	71	38	8	424
NonOPM58	D02	SCBI	Smithsonian Conservation Biol	2BC	179 -- 200	189.5	89	-97	11.6	0.72	72	5.8	5515	1517	56362	3286	61877	4803	68	57	11	0	86	55	3	95	1	0	64	0	1	19
NonOPM59	D10	RMNP	Rocky Mountain National Park	A	0 -- 10	5	90	-577	2.9	0.51	32	6.0	4350	1744	3018	668	7368	2411	470	461	9	192	33	117	343	25	61	4	352	288	14	515
NonOPM60	D10	RMNP	Rocky Mountain National Park	AB	10 -- 33	21.5	91	-577	2.9	0.51	26	6.1	4961	1644	2797	529	7758	2172	121	118	4	29	25	26	91	22	24	2	106	38	2	122
NonOPM61	D06	KONZ	Konza Prairie Biological Statio	A	0 -- 10	5	96	-634	12.4	0.38	95	6.7	4957	2360	4933	1459	9889	3819	408	397	10	43	96	233	164	59	28	2	244	955	107	3666
NonOPM62	D06	KONZ	Konza Prairie Biological Statio	Bt1	10 -- 26	18	97	-634	12.4	0.38	95	6.5	5216	3155	6043	1574	11259	4729	270	264	6	23	89	94	170	36	13	2	105	210	30	1562
NonOPM63	D06	KONZ	Konza Prairie Biological Statio	Bt2	26 -- 66	46	98	-634	12.4	0.38	97	7.8	5157	2921	6876	1676	12033	4597	210	202	8	12	100	129	60	64	9	1	129	120	22	57334
NonOPM64	D06	KONZ	Konza Prairie Biological Statio	Btkss	66 -- 89	77.5	99	-634	12.4	0.38	97	8.4	5346	1950	6308	1417	11654	3367	213	167	46	4	97	114	53	68	3	0	117	158	75	2122
NonOPM65	D06	KONZ	Konza Prairie Biological Statio	Btkv	89 -- 132	110.5	100	-634	12.4	0.38	93	8.1	5021	1611	4649	1108	9670	2719	230	120	109	2	94	80	41	66	2	0	85	32	25	651
NonOPM66	D06	KONZ	Konza Prairie Biological Statio	2BCv	132 -- 164	148	101	-634	12.4	0.38	88	8.2	5602	2114	5832	1103	11434	3218	161	89	72	3	89	79	10	89	3	0	90	26	14	88
NonOPM67	D06	KONZ	Konza Prairie Biological Statio	3Bt	164 -- 200	182	102	-634	12.4	0.38	89	8.1	5682	3087	1616	293	7298	3380	73	63	10	3	92	51	12	81	2	0	56	35	20	141
NonOPM68	D15	ONAQ	Onaqui	A1	0 -- 4	2	103	-1484	9	0.16	43	8.1	1051	1337	4370	531	5421	1868	161	154	7	15	49	67	86	44	11	1	138	29	3	168
NonOPM69	D15	ONAQ	Onaqui	A2	4 -- 12	8	104	-1484	9	0.16	41	8.5	786	1194	4383	480	5169	1674	62	58	4	5	57	56	2	96	5	1	98	12	1	6
NonOPM70	D15	ONAQ	Onaqui	Bw	12 -- 66	39	105	-1484	9	0.16	65	8.7	671	1077	5127	504	5798	1580	46	43	3	4	73	40	4	97	4	1	54	15	1	13
NonOPM76	D13	NIWO	Niwot Ridge Mountain Researc	A1	0 -- 14	7	111	-163	0.3	0.25	51	5.2	7218	3782	6082	837	13300	4619	714	700	15	61	39	249	451	36	63	7	646	99	8	733
NonOPM77	D13	NIWO	Niwot Ridge Mountain Researc	A2	14 -- 30	22	112	-163	0.3	0.25	38	5.2	6916	4158	6449	826	13364	4984	412	399	13	32	39	172	227	43	44	5	437	52	4	374
NonOPM78	D13	NIWO	Niwot Ridge Mountain Researc	Bw1	30 -- 49	39.5	113	-163	0.3	0.25	19	5.3	6211	3170	5256	445	11468	3615	157	151	7	11	18	56	95	37	27	3	308	13	1	116
NonOPM79	D13	NIWO	Niwot Ridge Mountain Researc	Bw2	49 -- 79	64	114	-163	0.3	0.25	28	5.5	5957	2983	7965	578	13922	3561	63	59	4	5	34	49	9	84	8	1	147	7	0	14
NonOPM80	D09	NOGP	Northern Great Plains Researcl	A1	0 -- 4	2	117	-780	5.9	0.42	83	7.2	3124	1721	6672	1482	9796	3203	532	524	8	63	79	290	234	55	29	2	368	297	25	1107
NonOPM81	D09	NOGP	Northern Great Plains Researcl	A2	4 -- 11	7.5	118	-780	5.9	0.42	83	6.9	3177	1828	7222	1646	10399	3473	467	458	9	48	84	292	167	64	28	3	346	305	29	1063
NonOPM82	D09	NOGP	Northern Great Plains Researcl	A3	11 -- 31	21	119	-780	5.9	0.42	82	6.9	3484	2026	7214	1168	10699	3193	325	321	4	27	87	242	79	75	21	2	277	211	24	623
NonOPM83	D09	NOGP	Northern Great Plains Researcl	Bt1	31 -- 46	38.5	120	-780	5.9	0.42	80	7.4	3612	2273	7828	1157	11440	3429	236	233	3	13	87	169	64	73	10	1	195	99	8	488
NonOPM84	D09	NOGP	Northern Great Plains Researcl	Bt2	46 -- 64	55	121	-780	5.9	0.42	78	7.7	4118	2360	8576	1183	12694	3544	237	235	2	10	83	171	64	73	8	1	206	59	4	375
NonOPM85	D09	NOGP	Northern Great Plains Researcl	Bt3	64 -- 84	74	122	-780	5.9	0.42	71	8.4	3567	1762	8387	1156	11954	2918	158	156	3	6	75	124	31	80	6	1	165	24	1	127
NonOPM86	D09	NOGP	Northern Great Plains Researcl	Btk1	84 -- 112	98	123	-780	5.9	0.42	74	8.7	2530	1150	8561	849	11091	1998	157	154	2	5	86	45	109	29	4	0	52	36	4	794
NonOPM87	D09	NOGP	Northern Great Plains Researcl	Btk2	112 -- 145	128.5	124	-780	5.9	0.42	71	8.9	3647	952	7586	740	11233	1692	139	136	3	3	80	57	79	42	3	0	71	20	1	396
NonOPM88	D09	NOGP	Northern Great Plains Researcl	Bk	145 -- 182	163.5	125	-780	5.9	0.42	70	9.0	3250	798	8767	706	12017	1504	143	136	7	3	78	58	78	43	3	0	74	14	1	361
NonOPM89	D05	UNDE	UNDERC	A	0 -- 8	4	127	-73	4.3	0.70	38	5.9	5446	4007	5590	359	11036	4365	261	255	6	40	41	131	123	52	41	4	321	67	4	209
NonOPM90	D05	UNDE	UNDERC	Bs	8 -- 15	11.5	128	-73	4.3	0.70	37	5.6	6381	4433	6037	327	12418	4760	140	135	5	20	41	58	77	43	17	2	141	34	2	131
NonOPM91	D05	UNDE	UNDERC	E	15 -- 23	19	275	-73	4.3	0.70	52	5.6	4436	3025	5223	225	9659	3249	56	52	4	14	54	45	7	86	11	1	83	30	2	16
NonOPM92	D05	UNDE	UNDERC	BS1	23 -- 31	27	129	-73	4.3	0.70	46	5.5	7127	6715	5933	362	13059	7077	121	115	6	15	50	57	58	50	10	1	114	30	2	115
NonOPM93	D05	UNDE	UNDERC	BS2	31 -- 48	39.5	130	-73	4.3	0.70	44	5.7	3700	3695	4904	200	8604	3895	50	48	2	6	50	24	24	51	5	0	48	12	1	47
NonOPM94	D05	UNDE	UNDERC	E/Bx	48 -- 57	52.5	131	-73	4.3	0.70	81	5.9	3733	1644	10940	641	14673	2286	743	742	1	1	78	19	723	3	1	0	24	4	1	3217
NonOPM95	D05	UNDE	UNDERC	2Bt1	57 -- 83	70	132	-73	4.3	0.70	91	6.3	2617	1529	12916	827	15533	2356	737	735	1	1	94	22	714	3	1	0	23	16	8	11704
NonOPM96	D05	UNDE	UNDERC	2Bt2	83 -- 114	98.5	133	-73	4.3	0.70	92	6.4	2373	1451	13237	759	15610	2210	726	725	1	1	91	155	571	21	1	0	171	11	3	6046
NonOPM97	D06	KONA	Konza Prairie Biological Statio	Ap	0 -- 12	6	136	-681	12.7	0.40	95	7.9	2796	2208	5237	1280	8033	3488	199	190	9	19	97	134	56	70	13	1	138	667	99	1992
NonOPM98	D06	KONA	Konza Prairie Biological Statio	Bt1	12 -- 31	21.5	137	-681	12.7	0.40	96	7.2	3530	2897	6149	1674	9679	4572	191	184	7	17	96	117	67	63	13	1	121	449	74	1794
NonOPM99	D06	KONA	Konza Prairie Biological Statio	Bt2	31 -- 54	42.5	138	-681	12.7	0.40	97	6.8	3934	3000	6289	1872	10223	4872	143	138	5	8	97	99	38	72	8	1	102	390	96	1373
NonOPM100	D06	KONA	Konza Prairie Biological Statio	Bt3	54 -- 89	71.5	139	-681	12.7	0.40	97	7.0	3567	2115	7000	2478	10567	4593	105	101	4	6	94	84	17	83	3	0	89	97	32	224
NonOPM101	D06	KONA	Konza Prairie Biological Statio	Btss	89 -- 119	104	140	-681	12.7	0.40	98	7.7	2893	2107	7546	1830	10440	3936	118	113	5	4	96	92	20	82	4	0	96	109	60	557
NonOPM102	D06	KONA	Konza Prairie Biological Statio	Btkss	119 -- 156	137.5	141	-681	12.7	0.40	97	8.3	2387	1715	7195	1449	9582	3164	143	136	7	4	100	129	3	95	2	1	129	146	84	1069
NonOPM103	D06	KONA	Konza Prairie Biological Statio	Btk	156 -- 206	181	142	-681	12.7	0.40	95	8.3	2406	1609	6777	1387	9183	2996	133	126	7	2	96	109	18	86	4	0	113	48	44	434
NonOPM104	D06	UKFS	The University of Kansas Field	A1	0 -- 13	6.5	143	-476	12.7	0.45	92	7.9	6830	2115	11306	1473	18136	3588	635	624	11	70	93	592	32	95	52	5	638	951	111	442
NonOPM105	D06	UKFS	The University of Kansas Field	A2	13 -- 28	20.5	144	-476	12.7	0.45	91	7.8	7803	2407	12599	1611	20401	4017	424	417	7	45	95	403	14	97	34	3	426	841	105	260
NonOPM106	D06	UKFS	The University of Kansas Field	Bt1	28 -- 43	35.5	145	-476	12.7	0.45	91	7.8	7759	2617	13567	1654	21326	4271	375	370	5	33	95	368	2	99	27	3	387	658	86	42
NonOPM107	D06	UKFS	The University of Kansas Field	Bt2	43 -- 76	59.5	146	-476	12.7	0.45	90	8.1	6570	2635	14024	1686	20593	4321	308	303	6	24	100	285	17	94	10	2	286	8954	1416	6550
NonOPM110	D13	MOAB	Moab	A	0 -- 6	3	151	-1484	10.1	0.15	27	6.7	1061	1020	3116	320	4177	1340	75	72	3	6	31	52	20	72	7	1	165	9	1	29
NonOPM111	D13	MOAB	Moab	Bw	6 -- 31	18.5	152	-1484	10.1	0.15	29	8.5	795	961	3479	316	4274	1277	70	68	2	3	34	66	2	96	6	1	194	5	1	4
NonOPM120	D01	BART	Bartlett Experimental Forest	A	3 -- 5	4	167	392	6.2	0.74	53	3.8	2485	1979	888	140	3373	2119	1795	1738	57	386	10	20	1718	1	17	1	200	428	17	1905
NonOPM121	D01	BART	Bartlett Experimental Forest	E	5 -- 9	7	168	392	6.2	0.74	41	5.0	4981	2896	2049	373	7031	3269	253	232	21	59	41	65	166	28	22	1	160	100	6	282
NonOPM122	D01	BART	Bartlett Experimental Forest	Bs1	9 -- 15	12	169	392	6.2	0.74	38	5.4	9949	15752	5028	1114	14976	16866	250	153	97	38	44	147	6	96	39	2	330	68	4	11
NonOPM123	D01	BART	Bartlett Experimental Forest	Bs2	15 -- 22	18.5	170	392	6.2	0.74	37	5.4	6641	11761	4030	898	10670	12659	195	128	67	27	35	82	47	64	35	2	230	42	3	72
NonOPM124	D01	BART	Bartlett Experimental Forest	Bw	22 -- 40	31	171	392	6.2	0.74	35	5.3	5783	7116	2620	475	8403	7590	112	78	33	13	36	62	17	79	17	1	170	20	2	26
NonOPM125	D01	BART	Bartlett Experimental Forest	BC	40 -- 73	56.5	172	392	6.2	0.74	29	5.4	5229	5082	1668	245	6897	5327	80	58	22	9	31	44	14	76	11	1	140	13	1	20
NonOPM126	D08	LENO	Lenoir Landing	A	2 -- 8	5	176	-147	18.1	0.51	54	5.8	6025	1462	3433	768	9457	2230	322	313	9	64	54	195	117	63	42	3	360	140	7	256
NonOPM127	D08	LENO	Lenoir Landing	Bw	8 -- 21	14.5	177	-147	18.1	0.51	49	5.2	5702	1449	3140	665	8842	2113	117	113	4	11	52	88	25	78	11	1	170	23	2	52
NonOPM128	D08	LENO	Lenoir Landing	Bg1	21 -- 58	39.5	178	-147	18.1	0.51	65	4.9	8739	2736	3838	785	12577	3521	80	73	6	8	61	67	6	91	7	1	110	20	2	16
NonOPM130	D08	LENO	Lenoir Landing	Bg3	102 -- 147	124.5	180	-147	18.1	0.51	81	4.9	10614	3142	5510	1101	16125	4242	93	78	15	7	81	32	46	41	4	1	40	36	5	240
NonOPM131	D08	LENO	Lenoir Landing	Bg4	147 -- 200	173.5	181	-147	18.1	0.51	92	4.9	12148	3826	7724	1412	19873	5238	112	93	19	9	88	38	55	41	5	1	43	74	10	456
NonOPM132	D07	GRSM	Great Smoky Mountains Natio	A1	0 -- 21	10.5	182	133	13.1	0.63	47	5.2	6519	7519	7627	1824	14146	9343	369	356	13	66	44	148	208	42	68	5	338	117	8	369
NonOPM133	D07	GRSM	Great Smoky Mountains Natio	A2	21 -- 32	26.5	183	133	13.1	0.63	44	5.5	7409	6539	9227	1792	16635	8330	146	102	44	19	52	75	27	74	20	2	143	40	3	56
NonOPM134	D07	GRSM	Great Smoky Mountains Natio	Bw	32 -- 58	45	184	133	13.1	0.63	45	5.1	8311	5019	8517	1361	16828	6380	116	64	52	8	47	41	23	64	8	1	87	15	2	43
NonOPM135	D07	GRSM	Great Smoky Mountains Natio	C	58 -- 100	79	185	133	13.1	0.63	27	5.2	5960	3489	7507	849	13466	4338	71	43	28	2	28	19	24	45	5	1	69	3	1	33
NonOPM136	D07	GRSM	Great Smoky Mountains Natio	Bw1	100 -- 140	120	186	133	13.1	0.63	63	5.2	8721	3999	10100	1516	18821	5516	123	45	78	2	64	30	15	66	2	1	46	5	2	42
NonOPM137	D07	GRSM	Great Smoky Mountains Natio	Bw2	140 -- 206	173	187	133	13.1	0.63	53	5.3	8449	4309	10493	1471	18942	5780	83	39	45	2	57	36	2	94	3	1	64	5	1	5
NonOPM138	D16	ABBY	Abby Road	A	3 -- 19	11	189	1394	10	0.75	73	5.5	11958	18174	41403	6244	53361	24418	385	361	23	128	75	229	132	63	71	4	305	513	23	532
NonOPM139	D16	ABBY	Abby Road	AB	19 -- 44	31.5	190	1394	10	0.75	75	5.3	10273	18189	43418	6851	53692	25040	289	219	70	22	84	185	34	84	36	3	221	133	8	208
NonOPM140	D16	ABBY	Abby Road	Bw1	44 -- 74	59	191	1394	10	0.75	80	5.2	9500	13853	50549	8073	60049	21926	247	227	20	49	86	188	39	83	15	1	219	348	21	277
NonOPM141	D16	ABBY	Abby Road	2Bw2	74 -- 103	88.5	192	1394	10	0.75	85	5.1	7916	5321	68832	7724	76748	13046	244	78	166	3	90	74	4	95	3	0	83	29	6	38
NonOPM142	D16	ABBY	Abby Road	2BC	103 -- 131	117	193	1394	10	0.75	79	5.2	7203	4801	72337	7078	79540	11879	214	72	141	2	90	70	2	97	2	0	78	20	5	21
NonOPM143	D08	TALL	Talladega National Forest	A1	0 -- 10	5	195	-116	17.2	0.56	9	5.0	1710	1024	3376	276	5087	1300	75	69	5	24	8	15	54	22	36	2	191	26	1	59
NonOPM144	D08	TALL	Talladega National Forest	A2	10 -- 25	17.5	196	-116	17.2	0.56	11	5.3	1771	1131	3227	313	4998	1444	56	52	4	9	10	19	33	37	17	2	194	10	1	36
NonOPM145	D08	TALL	Talladega National Forest	BE	25 -- 37	31	197	-116	17.2	0.56	12	5.3	1554	1153	2862	399	4417	1552	46	42	3	3	11	11	32	25	7	1	93	3	1	36
NonOPM146	D08	TALL	Talladega National Forest	Bt	37 -- 75	56	198	-116	17.2	0.56	22	4.8	2014	1476	6933	656	8947	2133	62	40	22	2	19	15	25	38	4	1	81	2	1	31
NonOPM147	D08	TALL	Talladega National Forest	Bc	75 -- 93	84	199	-116	17.2	0.56	12	5.0	1487	1283	4065	410	5552	1693	54	39	14	1	11	11	29	27	5	1	100	1	1	32
NonOPM148	D07	ORNL	Oak Ridge	A	1 -- 10	5.5	203	62	14.4	0.74	71	5.9	2610	2958	6671	1373	9281	4331	204	194	9	38	70	115	80	59	26	1	163	127	8	268
NonOPM149	D07	ORNL	Oak Ridge	E	10 -- 19	14.5	204	62	14.4	0.74	73	5.5	2497	2748	6715	1350	9213	4098	103	82	21	10	73	46	36	56	7	1	63	37	2	134
NonOPM150	D07	ORNL	Oak Ridge	Bt1	19 -- 40	29.5	205	62	14.4	0.74	76	5.3	3352	2322	8950	1501	12301	3823	82	63	19	2	73	59	5	93	2	0	80	7	1	17
NonOPM151	D07	ORNL	Oak Ridge	2Bt2	40 -- 65	52.5	206	62	14.4	0.74	76	5.3	4110	2125	13503	1682	17613	3808	95	44	51	4	69	41	3	92	2	0	59	13	1	11
NonOPM152	D07	ORNL	Oak Ridge	2Bt3	65 -- 147	106	207	62	14.4	0.74	81	5.0	2900	1871	32006	2425	34906	4296	160	48	112	1	86	43	5	89	1	0	50	7	2	37
NonOPM153	D07	ORNL	Oak Ridge	2Bt4	147 -- 180	163.5	208	62	14.4	0.74	78	5.1	3749	2131	27708	2157	31457	4289	169	51	118	1	82	47	4	92	2	0	57	5	2	24
NonOPM154	D02	SERC	Smithsonian Environmental Re	A	2 -- 13	7.5	210	-305	13.6	0.85	38	6.3	3884	2550	3595	636	7480	3186	195	189	6	33	40	97	92	51	38	2	242	55	3	154
NonOPM155	D02	SERC	Smithsonian Environmental Re	EA	13 -- 23	18	211	-305	13.6	0.85	38	5.9	4344	2588	3894	756	8238	3344	71	67	4	8	40	56	11	83	10	1	140	13	1	18
NonOPM156	D02	SERC	Smithsonian Environmental Re	E	23 -- 37	30	212	-305	13.6	0.85	39	5.4	5312	2426	4072	760	9384	3186	53	47	5	2	39	27	21	56	4	1	68	3	0	34
NonOPM157	D02	SERC	Smithsonian Environmental Re	Bt1	37 -- 60	48.5	213	-305	13.6	0.85	47	5.3	11048	3862	6637	1202	17685	5064	64	49	15	3	45	34	15	70	6	1	77	5	1	27
NonOPM158	D02	SERC	Smithsonian Environmental Re	Bt2	60 -- 75	67.5	214	-305	13.6	0.85	47	5.2	11616	3083	5718	920	17334	4004	49	28	21	2	44	22	5	80	3	1	51	4	0	10
NonOPM159	D02	SERC	Smithsonian Environmental Re	Bt3	75 -- 85	80	215	-305	13.6	0.85	49	5.1	19091	3007	14622	1235	33712	4241	76	42	34	2	50	34	8	81	3	0	68	4	0	16
NonOPM162	D07	MLBS	Mountain Lake Biological Stati	A	11 -- 44	27.5	223	143	8.8	0.82	21	4.3	956	2091	164	61	1120	2152	85	81	4	33	25	44	37	54	78	3	176	44	2	50
NonOPM166	D14	SRER	Santa Rita Experimental Range	A	0 -- 5	2.5	229	-2225	19.3	0.15	26	8.5	653	637	4598	376	5251	1013	100	97	3	3	31	39	58	40	5	1	124	4	1	85
NonOPM167	D14	SRER	Santa Rita Experimental Range	Bw	5 -- 41	23	230	-2225	19.3	0.15	36	8.6	336	682	4538	382	4874	1064	44	37	7	3	51	30	7	81	5	1	59	6	2	14
NonOPM168	D14	SRER	Santa Rita Experimental Range	Bk1	41 -- 79	60	231	-2225	19.3	0.15	31	8.6	309	514	3561	288	3870	802	41	34	6	4	38	18	16	54	5	0	48	6	1	26
NonOPM169	D14	SRER	Santa Rita Experimental Range	Bk2	79 -- 132	105.5	232	-2225	19.3	0.15	23	8.5	428	390	3365	250	3794	640	52	26	26	1	29	13	14	49	3	1	44	1	1	19
NonOPM170	D14	SRER	Santa Rita Experimental Range	2Bk	132 -- 203	167.5	233	-2225	19.3	0.15	41	8.4	328	545	5586	372	5913	917	34	27	7	0	47	25	2	93	3	0	53	0	1	4
NonOPM171	D05	STEI	Steigerwaldt Land Services	A	0 -- 14	7	234	-100	4.8	0.69	50	5.2	5039	2214	3606	372	8645	2586	169	162	7	34	50	88	74	54	28	2	176	67	4	148
NonOPM172	D05	STEI	Steigerwaldt Land Services	Bs1	14 -- 28	21	235	-100	4.8	0.69	50	5.1	7414	4222	3736	426	11151	4648	113	96	18	16	52	54	41	57	15	1	105	33	2	86
NonOPM173	D05	STEI	Steigerwaldt Land Services	Bs2	28 -- 36	32	236	-100	4.8	0.69	48	5.1	6144	4379	3670	384	9814	4763	61	47	14	10	53	34	13	73	10	1	65	21	1	27
NonOPM178	D19	DEJU	Delta Junction	A	5 -- 16	10.5	243	-324	-3	0.37	66	5.1	10879	6415	11400	1088	22280	7504	136	125	11	27	67	58	67	46	12	1	87	80	4	199
NonOPM200	D05	TREE	Treehaven	A/E	2 -- 17	9.5	277	-103	4.8	0.72	30	5.4	4833	2246	4349	407	9182	2653	138	131	7	23	32	61	70	47	26	2	192	34	2	102
NonOPM204	D17	TEAK	Lower Teakettle	A1	0 -- 19	9.5	285	-461	8	0.60	20	5.7	4661	7757	1732	618	6394	8375	145	141	4	52	27	54	87	38	35	3	197	72	3	120
NonOPM205	D17	TEAK	Lower Teakettle	A2	19 -- 43	31	286	-461	8	0.60	20	5.5	5073	9163	1838	603	6912	9766	59	58	1	24	22	55	3	95	38	2	251	31	2	3
NonOPM206	D17	TEAK	Lower Teakettle	A2	43 -- 67	55	287	-461	8	0.60	21	5.2	5128	9958	1890	646	7018	10605	113	106	7	30	24	55	51	52	38	3	234	39	2	66
NonOPM207	D17	TEAK	Lower Teakettle	A3	67 -- 101	84	288	-461	8	0.60	21	5.4	4996	8763	1822	565	6817	9329	66	63	3	20	24	63	0	100	38	3	257	26	1	0
NonOPM208	D17	TEAK	Lower Teakettle	2AC	101 -- 132	116.5	289	-461	8	0.60	21	5.3	4912	9344	1656	530	6568	9874	67	62	5	18	21	58	4	93	37	3	271	23	1	6
NonOPM209	D17	SJER	San Joaquin Experimental Ran	A1	0 -- 8	4	294	-1574	16.4	0.54	21	5.4	1964	1407	1333	259	3296	1667	76	74	1	12	25	43	31	58	16	2	171	16	1	42
NonOPM213	D16	WREF	Wind River Experimental Fore	Ac	9 -- 50	29.5	303	1138	9.2	0.79	51	5.4	8286	12918	11246	3725	19532	16643	166	114	52	15	67	85	29	74	10	1	127	45	3	88
NonOPM214	D16	WREF	Wind River Experimental Fore	Bw	50 -- 80	65	304	1138	9.2	0.79	54	5.5	9760	18026	11245	3535	21006	21561	336	198	138	12	68	191	7	97	8	1	282	37	3	20
NonOPM215	D16	WREF	Wind River Experimental Fore	BC	80 -- 94	87	305	1138	9.2	0.79	45	5.8	12150	28560	7983	2241	20134	30801	722	247	475	5	68	244	2	99	6	1	362	15	2	7
NonOPM216	D16	WREF	Wind River Experimental Fore	2C1	94 -- 136	115	306	1138	9.2	0.79	22	5.7	11336	36789	3101	1012	14438	37801	836	322	514	4	42	319	4	99	9	1	759	7	1	7
NonOPM217	D16	WREF	Wind River Experimental Fore	2C2	136 -- 162	149	307	1138	9.2	0.79	11	5.7	8862	38010	667	230	9529	38240	665	326	339	3	28	322	3	99	9	1	1155	4	1	5
NonOPM218	D16	WREF	Wind River Experimental Fore	3AB	162 -- 178	170	308	1138	9.2	0.79	13	5.7	8366	30898	669	251	9035	31149	493	185	308	5	32	182	3	99	13	1	567	7	1	4
NonOPM219	D19	HEAL	Healy	A/Cjj	31 -- 50	40.5	311	-209	-1.3	0.30	65	5.0	9151	2535	1948	664	11099	3199	964	957	7	96	57	112	845	12	36	1	197	221	9	1952
NonOPM220	D19	HEAL	Healy	Cjjf	50 -- 84	67	312	-209	-1.3	0.30	61	5.2	8311	2168	2266	686	10577	2853	541	535	6	53	63	102	433	19	33	1	162	142	5	1167
NonOPM221	D19	BONA	Caribou-Poker Creeks Researc	Bg/Oajj	22 -- 38	30	313	-367	-3	0.43	74	5.1	16519	2589	4911	625	21430	3214	243	236	7	49	76	110	126	47	26	2	146	200	8	516
NonOPM222	D19	BONA	Caribou-Poker Creeks Researc	Cg	38 -- 56	47	314	-367	-3	0.43	82	5.4	9920	2326	4613	808	14533	3134	170	162	8	32	85	107	55	66	20	1	126	206	8	357
NonOPM227	D18	BARR	Barrow Environmental Observ	Cgjj/Oajj	32 -- 45	38.5	319	-122	-12	0.07	62	5.8	9835	2257	2137	961	11971	3218	1000	948	53	109	60	445	502	47	65	5	741	272	15	1259
NonOPM228	D18	BARR	Barrow Environmental Observ	Oaf/Cgjjf	58 -- 110	84	320	-122	-12	0.07	47	6.3	9887	1721	1764	762	11651	2483	632	619	13	88	44	217	402	35	47	3	498	155	8	712
NonOPM229	D12	YELL	12_YELL_Pit1_Archive_0-4_A	A_1	0-4	2	322	-674	3.4	0.33	64	6.8	4213	1890	6501	1185	10715	3075	629	623	6	93	57	295	329	47	39	1	520	214	17	759
NonOPM230	D12	YELL	12_YELL_Pit1_Archive_4-29	Bt1_1	4-29	16.5	323	-674	3.4	0.33	61	6.6	5271	2250	8317	1443	13588	3693	222	219	3	31	69	215	4	98	18	2	313	99	9	13
NonOPM231	D12	YELL	12_YELL_Pit1_Archive_29-45	Bw_1	29-45	37	324	-674	3.4	0.33	61	7.1	4713	2413	8517	1461	13230	3873	165	163	2	24	61	116	47	71	16	1	189	62	5	121
NonOPM232	D12	YELL	12_YELL_Pit1_Archive_45-67	Bt2_1	45-67	56	325	-674	3.4	0.33	61	7.4	4431	2371	8541	1526	12972	3897	141	139	2	15	66	103	36	74	12	1	157	43	3	105
NonOPM237	D20	PUUM	D20_PUUM_Pit1_ARCHIVE	Bw1_1	17-59	38	330	1440	12.7	0.97	45	5.3	36290	22507	2723	202	39013	22709	1535	1475	60	175	29	349	1126	24	115	12	1214	245	16	1581
NonOPM238	D20	PUUM	D20_PUUM_Pit1_ARCHIVE	2Bw2_1	59-90	74.5	331	1440	12.7	0.97	52	5.4	39003	51929	7122	521	46125	52450	1509	1341	168	156	42	536	804	40	116	8	1285	267	17	1380